MEASUREMENT, COMPARISON, AND USE OF REMOTELY DERIVED LEAF AREA INDEX PREDICTORS

By

RYAN R. JENSEN

A DISSERTATION PRESENTED TO THE GRADUATE SCHOOL
OF THE UNIVERSITY OF FLORIDA IN PARTIAL FULFULLMENT
OF THE REQUIREMENTS FOR THE DEGREE OF
DOCTOR OF PHILOSOPHY

UNIVERSITY OF FLORIDA

2000

ACKNOWLEDGMENTS

A dissertation is never the result of one person's efforts. Rather, it is the culmination of many people working together for a common goal. I wish to thank my committee members, Peter Waylen, Nigel Smith, and Francis Putz for teaching me how to conduct research and write a dissertation. I would especially like to thank my committee chair, Michael Binford, for providing me with the guidance, freedom, and knowledge to complete this dissertation.

My family has been instrumental in allowing me to complete this work. My wife, Tricia, and my two daughters, Savannah and Sierra, have suffered patiently through many days when dad was either away doing fieldwork, or worse, typing on the computer in our living room. Thank you girls! I would also like to thank my father, John Jensen, for reviewing this work many times. Finally, I would like to thank the office staff and my fellow graduate students for their support.

TABLE OF CONTENTS

page

ACKNOWLEDGEMENTS ii

ABSTRACT v

CHAPTERS

1 INTRODUCTION 1

2 STUDY AREA 9

Longleaf Pine / Turkey Oak Sandhills 9
Sand Pine Scrub 13
Hammocks 14
Other North Florida Communities 15

3 BACKGROUND AND LITERATURE REVIEW 16

Biophysical Rationale 16
Remote Sensing of Vegetation 16
Leaf Area Index 24
Vegetation Indices 26
LAI and Remote Sensing Vegetation Indices 29
Artificial Neural Networks 30
Network Architecture 33
Network Training 35
Neural Networks and Remote Sensing 37
Satellite Imagery 38

4 METHODS 40

Goals 40
Hypotheses 40
Methods 42
Field LAI Measurements 42
Brightness Value Extraction 43
Multiple Regression of Six TM Spectral Bands 43
Vegetation Indices and LAI 44
Artificial Neural Network and LAI 44
Overall Accuracy 44

5 RESULTS 46

Regression Analyses 46

Artificial Neural Network 59
Overall Accuracy 70
Discussion 75

6 ECOLGOGICAL STUDIES 77

Leaf Area Index, Fire, and Succession in Longleaf Pine/Turkey Oak Sandhills 79
Comparisons of the Urban Forests in Gainesville and Ocala, FL 92

6 DISCUSSION AND CONCLUSION 106

Discussion 106
Other Sensors 108
Conclusions 110
Future Research 114

APPENDICES

A COMPUTATION OF LOCAL TASSELED CAP COEFFICIENTS 112

B GIS PROGRAM USED TO INTERPOLATE BRIGHTNESS VALUES 115

C CREATION OF LAI SURFACE IMAGES USING ANNS 121

REFERENCES 122

BIOGRAPHICAL SKETCH 133

Abstract of Dissertation Presented to the Graduate School
of the University of Florida in Partial Fulfillment of the
Requirements for the Degree of Doctor of Philosophy

MEASUREMENT AND COMPARISON OF REMOTELY DERIVED LEAF AREA INDEX PREDICTORS IN NORTH CENTRAL FLORIDA

By

Ryan R. Jensen

May 2000

Chair: Michael W. Binford
Major Department: Geography

Environmental change occurs in response to both natural and anthropogenic causes. As the world's human population continues to increase, anthropogenic change will also increase. These changes affect the health and vigor of forests throughout the world, including those in north central Florida. Leaf Area Index (LAI), the amount of leaf area per unit ground area, is an important biophysical variable that is directly related to rates of atmospheric gas exchange, biomass partitioning, and productivity. While global and local models that map biophysical parameters are prevalent in the literature, landscape to regional scale models are less common. Therefore, the ability to map and monitor LAI over landscape to regional scale areas is essential for understanding medium scale biophysical properties and how these properties affect biogeochemical cycling, biomass accumulation, and primary productivity. This study develops and verifies several new models to estimate LAI using *in situ* field measurements throughout north central Florida, Landsat Thematic Mapper remotely sensed imagery, remotely derived vegetation indices, simple and multiple regression, and artificial neural networks (ANNs). This study concludes that while multiple band regression and regression with

individual vegetation indices (Normalized Difference Vegetation Index, Soil Adjusted Vegetation Index, Simple Ratio, and Greenness Vegetation Index) can estimate LAI, the most accurate way to estimate regional scale LAI is to train an ANN using *in situ* LAI data and remote sensing brightness values measured from six different portions of the electromagnetic spectrum.

The new ANN method of estimating LAI is then applied to two forest ecology studies. The first study analyzes LAI in longleaf pine/turkey oak sandhills as a function of time since last burn. It concludes that in the absence of fire, sandhill LAI increases, and this may be useful for identifying where prescribed burns need to be done. The second study estimates and compares urban forest LAI in Ocala and Gainesville, Florida as a function of existing tree ordinances in the two cities. It concludes that Gainesville's urban forest has higher LAI values principally because of a very strict tree ordinance.

CHAPTER 1
INTRODUCTION

Environmental change occurs in response to both natural and anthropogenic events. Natural events include migration of continents, building and erosion of continents, sea level change, the El Niño-southern oscillation, hurricanes, tornados, fire, landslides, variations of solar intensity, and even meteor strikes. Anthropogenic events include land cover/land use conversion, increased carbon dioxide emission through fossil fuel burning and land conversion, and fire suppression (Curran and Foody, 1994). As the world's human population continues to grow, human-induced environmental change will increase. These events are often well studied at the local scale where observation and contemplation have occurred for millennia and at the global scale where significant amounts of research have been done since the early 1960s. However, this understanding rarely extends to the landscape and regional scales as it is based on limited research and lacks robust models and relevant data (Curran and Foody, 1994). Knowledge of biophysical characteristics of vegetation at the landscape and regional scales is necessary to describe energy and mass fluxes at the Earth's surface using global circulation models, carbon cycle models, and water models (Weiss and Baret, 1999). The need for such knowledge is now accepted (IGBP, 1990) and models must be developed that incorporate regional scale models (Curran, 1994).

Many of the ecological questions concerning the relationship between both natural and anthropogenic effects on the environment require accurate estimates of biophysical variables. Biophysical variables include ecosystem characteristics such as

primary production, total plant biomass, components of the nitrogen cycle, and evapotranspiration rates that describe ecosystem properties and functions (Aber and Melillo, 1991). A biophysical variable of principal importance is Leaf Area Index (LAI) defined as m^2 of leaf per m^2 of ground (Curran, 1994; Pierce and Running, 1998; Lymburner, L, P.J. Beggs and C.R. Jacobson., 2000). Leaves represent the fundamental photosynthetic organ of trees and other plants. Inputs to leaves include short- and long-wavelength radiation, water, and nutrients from the soil. Outputs include long-wavelength radiation, conduction and convection, transmission of light, transpiration, reflectance, and energy stored in carbon compounds (sugars) for export to the remainder of the plant (Aber and Melillo, 1991). Because leaves are the primary organs for canopy-atmosphere gas exchange, LAI is a key variable in atmospheric circulation models (Ruimy, A., B. Saugier, G. Dedieu, 1994). Leaves fix carbon dioxide (CO_2) during photosynthesis, and release CO_2 during respiration. The balance between the two is known as net carbon fixation and when extrapolated at the landscape scale this helps to explain large-scale carbon dynamics. One important way that biophysical variables, such as LAI, are measured at the landscape scale is through remote sensing.

Satellite remote sensing, defined as the measurement and analysis of earth phenomena from space, has been used in many vegetation studies (e.g., Bonan, 1993; Curran, 1994; Gong, Ruiliang, and Yu, 1997). Remotely sensed data from satellites possess a variety of attributes useful for large-scale vegetation mapping. For example, satellite remote sensing data provide a synoptic view of landscape- to regional-scale areas and are collected uniformly in space and time in a nondestructive manner (Green, Mumby, Edwards, Clark, and Ellis, 1997; Friedl and Brodley, 1997). Satellite remote

sensing can continuously monitor the earth's surface through orbiting platforms that contain sensors, which measure emitted or reflected energy (Aber and Melillo, 1991).

Despite its importance, knowledge of and ability to measure landscape-scale[1] LAI using remotely sensed data is limited because:

(i) Current methods of *in situ* LAI measurement are labor intensive, making it difficult to measure throughout large geographic areas, rendering use of these methods beyond the stand level impractical (Fassnacht, Gower, MacKenzie, Nordheim, and Lillesand, 1997).

(ii) Adequate spatial and temporal sampling is difficult to achieve using ground measurement techniques to monitor landscape scale LAI (Weiss and Baret, 1999).

(iii) Present-day field LAI data are difficult to relate to historical remote sensor data because forests change over the time elapsed between scene acquisition and LAI measurement. (Lillesand and Keifer, 1996; Jensen, 2000).

(iv) Standard methods for estimating LAI from satellite remote sensing data are inadequate across the range of LAI because some studies have found a threshold LAI value of 2 - 4 where commonly used vegetation indices fail to increase in relation to increased LAI values (e.g., the Normalized Difference Vegetation Index (Figure 1-1; Carlson and Ripley, 1997; Datt, 1998; Lawrence and Ripple, 1997).

Interception, scattering, and emission of electromagnetic radiation by leaves are closely related to forest canopy structure (Mather, 1987). If the spatial aspects of LAI

[1] Turner and Gardner (1991) define landscape as the landforms or ecosystems of a region in the aggregate, or to the land surface and its associated habitats at scales of hectares to many square kilometers.

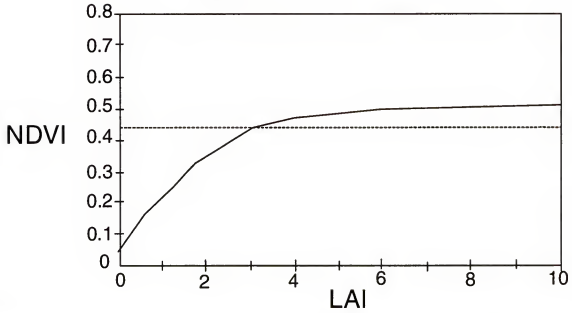

Figure 1-1. Leaf-Area-Index (LAI) saturation in relation to the Normalized Difference Vegetation Index (adapted from Carlson and Ripley, 1997).

can be inferred directly from the spectral characteristics of forests, many of the problems associated with obtaining landscape-scale LAI of forests could be avoided (Green et al., 1997). Better remote-sensing based estimates of LAI are required for large-scale, long-term understanding of landscape-scale ecosystem processes.

This research develops and evaluates several new approaches to estimate LAI by application of multivariate and univariate statistics, and artificial neural networks (ANN) to satellite remote sensor data, and compares the results to *in situ* LAI measured in forested ecosystems in north-central Florida. The coastal plain of the southeastern U.S. is an excellent physiographic region to develop better methods to estimate LAI because it contains some of the more rapidly changing forest ecosystems in North America. These ecosystems include longleaf pine/turkey oak sandhills, southern mixed hardwood forests, and sand pine scrub communities.

This study specifically compares the use of ANN analysis techniques with traditional statistics applied to remotely sensed data to estimate LAI of forested ecosystems. It builds upon previous research but proposes a more accurate estimation of LAI by using six of the seven Landsat Thematic Mapper (TM) spectral bands, and by integrating statistical analysis and ANN techniques into the estimation. The research determines the most accurate of these methods to estimate LAI with remotely sensed data, and then applies the methods to two forest-ecology issues. The first issue concerns the relationship between LAI and fire in longleaf pine/turkey oak sandhills. The second issue concerns the relationship between municipal tree policies and urban forest LAI.

This dissertation answers the following questions:

1. What are the most effective techniques for extracting LAI information from remotely sensed data?

Remote sensing systems can provide data for monitoring very large geographic areas through moderately long periods of time. Correlation and regression analyses are common methods used to relate *in situ* forest measurements with remotely sensed data from the same study area (Jensen and Qui, 2000). An analysis of different LAI estimation techniques applied to forests in the southeastern coastal plain would be a major contribution.

2. How do the accuracies of standard statistical analysis and vegetation index methods for estimating LAI compare with relatively new techniques such as Artificial Neural Networks (ANNs)?

Despite the popularity of ANNs, little research has been done that uses ANNs to estimate biophysical variables such as LAI (Jensen and Qui, 2000). ANNs are still somewhat new, and many scientists have not acquainted themselves with them, thus limiting their research questions that use ANNs. This study develops an ANN approach to estimating LAI.

This research will determine which of the methods presented in this proposal is the most accurate way to estimate LAI of landscape-scale areas in several southeastern coastal plain ecosystems of the U.S.A.. The techniques developed in this research should be applicable to other forests throughout the world provided *in situ* measurements of LAI are made in representative ecosystems.

3. Because ecosystems are constantly changing, how can the techniques developed in this research be applied to ecological LAI studies?

One of the major goals of conducting remote sensing research is to develop new methods that can be accurately applied to ecological studies (Fassnacht et al., 1998). Landscape-scale ecological studies that examine biophysical changes such as the relationships between fire and forest ecology, urban forestry and municipal government policies, and temporal and spatial forest changes are necessary to obtain a synoptic view of environmental change from the local to global scales.

Two ecological studies were completed using the techniques developed in this research. In the first study, LAI of burned and unburned longleaf pine/turkey oak sandhills are compared. Sandhills once comprised the most extensive ecosystem in the southeastern United States, but sandhill area has decreased markedly because of habitat fragmentation, urban development, and fire suppression (Carter, MacKenzie, and Gjerstad., 1999; Myers, 1990). Sandhills are dependent on fire for species regeneration and health maintenance. In the absence of fire, sandhills will usually succeed into southern mixed hardwood forests (Myers, 1990). This study quantifies LAI sandhill areas in Katharine Ordway Preserve as a function of time since last burn.

In the second application, the urban forests of Gainesville and Ocala, Florida are compared. Urban forests can reduce air pollution, energy consumption, and increase property values (Tyrvainen and Vaananen, 1998). Municipal tree policies can affect the urban forests. Gainesville has very strict tree ordinances that govern the types and number of trees that may be removed for development and the types and number of trees that must be replanted. Full-time arborists enforce this ordinance. Ocala has a weaker

tree ordinance that allows for more trees to be removed and fewer trees to be planted that is enforced by a committee of nine persons. The urban forest LAIs of these two cities is quantified and compared using the techniques developed in this study.

CHAPTER 2
STUDY AREA

The study areas used to test the four (4) hypotheses consist of forested ecosystems found throughout north-central Florida. North-central Florida is characterized by longleaf pine (*Pinus palustris*) and turkey oak (*Quercus laevis*) sandhills, sand pine (*P. clausa*) scrub, temperate hardwood forests (hammocks; Abrahamson and Hartnett, 1990), and other plant communities. This chapter identifies the characteristics of these communities including their soils, flora, climate, hydrology, fire frequency, historic land-use, and potential future land-use.

Longleaf Pine / Turkey Oak Sandhills

Longleaf pine / turkey oak (LLP/TO) sandhills were once one of the most widespread ecosystems in Florida (and the southeastern United States) until fire suppression, habitat degradation, logging, conversion to other southern pines (*P. elliotii* and *P. taeda*), clearing for crops, and habitat fragmentation reduced them to about 3% of their previous extent (Platt, 1998). Prior to European settlement they occupied up to 37 million ha in the southeastern U.S.A. (Brockway and Outcalt, 1998). Sandhill communities occur in areas of rolling terrain on deep, well-drained, white to yellow, sterile sands with almost no silt, clay, or organic matter (Myers, 1990), and are usually extremely nutrient poor. Because their soils are well drained, these communities are prime areas for development.

Sandhills occur in warm, temperate climates. These xeric communities contain overstories of longleaf pine with turkey oak and bluejack oak (*Q. incana*) in the understory. While sandhills typically have less tree species diversity than hammocks or other woody ecosystems, they contain more overall diversity because of an extremely species rich herbaceous layer that contains species such as green eyes (*Berlandiera subacaulis*), splitbeard blustem (*Andropogen Ternarius*), honeycomb head (*Balduina angustifolia*), and many others (Myers 1990). In fact, sandhill communities are the most species-rich habitats outside of the tropics (Carter et al., 1999). Sandhills in Florida often have a park-like appearance because of the seemingly continuous wiregrass (*Aristida beyrichiana*) ground cover (Figure 2-1).

Sandhills depend on regular fires (recurring every 1 – 10 years) for species reproduction and protection from invasion (Myers, 1990). Because of this relationship with fire, sandhill species have developed a dependence on fire that is unmatched by other tree-dominated communities in the state. For example, longleaf pine seedlings remain in what is known as the grass stage (Figure 2-2) for 5 to 20 years while storing large quantities of photosynthates in a deep tap root. The apical bud is embedded in the surrounding erectly displayed needles that are resistant to burning (Aber and Melillo, 1991). After a fire, the seedlings can grow as much as 1 meter in height per year. A decrease in fire frequency leads to an establishment of other pine and oak species. Therefore, oaks and other hardwoods now dominate many of the areas that were once LLP/TO sandhills.

Figure 2-1. Park-like appearance of longleaf pine/turkey oak sandhill with continuous ground cover of wiregrass.

Figure 2-2. Longleaf pine passing out of grass stage.

Many mammals are dependent on sandhills for their survival. Two particularly fire-dependent species, gopher tortoise (*Gopherus polyphemus*) and red cockaded woodpecker (*Picoides borealis*), are on the federally endangered species list (Myers, 1990). This research focused on sandhill communities in the Katharine Ordway Preserve, Ocala National Forest, and other publicly accessible lands.

Sand Pine Scrub

Sand pine scrub communities occur on sterile, well-drained sands deposited from former coastlines of ancient seas (Carter et al., 1998). The overstory is typically dominated by sand pine (*P. Clausa*) with a mixed understory normally consisting of myrtle oak (*Q. myrtifolia*), Chapman's oak (*Q. chapmanii*), sand live oak (*Q. geminata*), Florida rosemary (*Ceratiola ericoides*), and holly (*Ilex opaca*). Ground cover is sparse but typically consists of beak rush (*Rhynchospora megalocarpa*), milk peas (*Galactia spp.*), gopher apple (*Licania michauxii*), and various grasses (Myers, 1990). This ecosystem is endemic to Florida and occurs most extensively in Ocala National Forest, which features the world's largest scrub community.

Sand pine scrub communities develop in a warm temperate climate, and differences in microclimate are of little importance in stand structure (Myers, 1990). The water table never reaches the surface, and soil leaching results from rainfall. As a result, sand pine scrub is one of the driest ecosystem types in the region. Research suggests that, in contrast to many vegetation types in Florida, hydrology has less to do with species composition in scrub communities than fire and nutrient availability (Myers, 1990). Fire

is used as a management tool in these xeric communities and can result in large even-aged stands.

To many people, sand pine scrub communities are impenetrable areas of economically worthless trees on poor soils and are prime areas for clear cutting and human development (Myers, 1990). Because of this perspective extensive areas of scrub communities have been destroyed. This study examined sand pine scrub communities in the Ocala National Forest.

Hammocks

Temperate hardwood forests, or hammocks, exist sparsely throughout Florida. Historically, hammocks were narrow bands of vegetation, confined to slopes between upland sandhill pinelands and bottomland lake margins or floodplain forests. In northern Florida, hammocks contain the largest variety of tree species per unit area in the United States (Platt and Schwartz, 1990). Despite this diversity, there are several species that can be common including laurel oak (*Q. hemisphearica*), sabal palm (*Sabal palmetto*) Southern magnolia (*Magnolia grandiflora*,), basket oak *(Q. michauxii*), live oak (*Q. virginiana*), sweet gum (*Liquidambar styraciflua*), spruce pine (*P. glabra*), and pignut hickory (*Carya glabra*) (Platt and Schwartz, 1990). Hardwood hammocks occur on clay-rich soils and calcareous slopes, or alluvial clay soils and sands (Platt and Schwartz, 1990). Soils that support hammocks are the most fertile in the state. Local soils are affected by a number of biotic and abiotic factors such as hydrology, fire, slope, and flora and fauna interactions.

Hammocks generally occur where fire has been absent for a long time (Platt and Schwartz, 1990), and develop in a variety of climates that help shape species structure.

For example, susceptibility to freezing decreases the number of tropical trees in hammocks, while the violent nature of Florida's weather (e.g., thunderstorms and hurricanes) increases the diversity of some hammocks. The spatial extent of hammocks has in increased because of fire suppression and other factors and now totals 16 to 18% of Florida's forested land (Platt and Schwartz, 1990). This study examined hammocks in the San Felasco Hammock State Reserve and other State lands throughout north central Florida.

Other North Florida Communities

Although north Florida contains other forested communities such as swamps, mangroves, and pine flatwoods, LAI in these ecosystems was not measured for this project primarily because these communities have long hydroperiods (Ewel, 1990). While not impossible, it is difficult to determine the leaf-area-index and many other biophysical parameters when the instantaneous field of view (IFOV) of the sensor system collects spectral information consisting of very wet hydric soils and vegetation (Jensen, 2000).

CHAPTER 3
BACKGROUND AND LITERATURE REVIEW

Biophysical Rationale

The techniques and theory underlying this research have been under development for many years. This chapter places this research project in the context of what has already been done on remote sensing and leaf area index (LAI) and what is understood from these studies. First, the physics of remote sensing vegetation are described. Then, the concept of LAI is summarized followed by a description of remotely derived vegetation indices and how the two are related. Next, artificial neural networks are described. Finally, the Landsat Thematic Mapper, the remote sensing system used in this research is detailed.

Remote Sensing of Vegetation

Forest canopy structure is the spatial arrangement of leaves, branches, and stems. Leaves serve as both solar energy collectors and gas exchangers. Stems and branches support these exchange surfaces in such a way that radiative and convective exchange can occur in an efficient manner. Canopy structure affects radiative and convective exchange of tree stands, so information about canopy structure is necessary for modeling these processes (Jensen, 2000). Remote sensing of vegetation provides a means to obtain this information.

The sun emits radiant energy over most of the electromagnetic spectrum. Some of this energy is absorbed, particularly in wavelengths associated with water vapor and major atmospheric gases when passing through Earth's atmosphere. Leaves reflect some of this incoming energy, but absorb most. Only the energy in a very narrow set of wavelengths in the visible part of the spectrum (0.35 – 0.70 μm) is converted by chlorophyll in chloroplasts into simple sugars that are the first products of photosynthesis (Aber and Mellilo, 1991).

Healthy green leaves intercept incident radiant flux (Φ_I) directly from the Sun or diffuse, scattered skylight. This energy interacts with the water, pigments, and intercellular air spaces within the leaf in several ways, including serving as the energy source for photosynthesis. The amount of radiant flux reflected by the leaf (Φ_r), absorbed by the leaf (Φ_α), and transmitted through the leaf (Φ_τ) can be measured by applying an energy balance equation to keep track of what happens to the incident radiation (Jensen, 2000). The general equation for the interaction of spectral (λ) radiant flux with the leaf is:

$$\Phi_{i_\lambda} = \Phi_{r_\lambda} + \Phi_{\alpha_\lambda} + \Phi_{\tau_\lambda}$$

Most remote sensing systems function in the 0.35 – 3.0 μm band of the electromagnetic spectrum, measuring primarily reflected energy. The energy in the bandwidth is finite, and is partitioned into reflected, absorbed, and transmitted components when it enters the forest canopy. The total radiation is decomposable into the different components by dividing each of the variables by the original radiation flux,

which gives the proportion in each component. Therefore, after dividing each of the variables by the original incident radiation flux Φ_{i_λ}:

$$\frac{\Phi_{i_\lambda}}{\Phi_{i_\lambda}} = \frac{\Phi_{r_\lambda}}{\Phi_{i_\lambda}} + \frac{\Phi_{a_\lambda}}{\Phi_{i_\lambda}} + \frac{\Phi_{\tau_\lambda}}{\Phi_{i_\lambda}}$$

yields:

$$i_\lambda = r_\lambda + \alpha_\lambda + \tau_\lambda$$

where r_λ is spectral reflectance by the leaf . α_λ is spectral absorbance, and τ_λ is spectral transmittance by the leaf. Solving for reflectance, r_λ , yields:

$$r_\lambda = i_\lambda - (\alpha_\lambda + \tau_\lambda)$$

where the energy reflected from the leaf surface is equal to the incident energy minus the energy absorbed by the plant for photosynthesis and the amount of energy transmitted through the leaf onto other leaves or the ground (Jensen, 2000).

Atmospheric conditions, absorbance, transmittance, and photosynthetic rate at the time of image acquisition determine how a leaf and the associated plant canopy appear radiometrically on remotely sensed images. The ability to measure and differentiate these radiometric properties allows for canopy studies to be conducted using remote sensing imager.

Photosynthesis requires carbon dioxide (CO_2), water (H_2O), and light:

$$6CO_2 + 6H_2O + lightenergy \longrightarrow C_6H_{12}O_6 + 6O_2$$

The CO_2 from the air and the water provided by the root and stem represent the fundamental raw materials of photosynthesis. Sunlight provides the energy to power photosynthesis (Campbell, 1996)

Molecules, when struck by a wave or photon of light, reflect a portion of the energy and absorb a portion of the energy, causing the molecules to enter into a higher energy state. Each compound absorbs or reflects its own characteristic wavelengths. Photosynthetic pigment molecules in green vegetation absorb primarily in the visible portion of the electromagnetic spectrum (0.35 – 0.70 μm; Figure 3-1). An absorption spectrum for a particular pigment describes the wavelengths at which it can absorb light and enter into an excited state. Chlorophyll *a* and *b* both absorb blue and red light: chlorophyll *a* peak absorbance is at wavelengths of 0.43 μm and 0.66 μm and chlorophyll *b* peak absorbance is at 0.45 μm and 0.65 μm (Jensen, 1983). A relative lack of absorption in the wavelengths between the two chlorophyll absorption bands produces a peak at 0.54 μm, in the green region. The two optimum spectral regions for sensing the chlorophyll absorption characteristics of a leaf are at 0.45 – 0.52 μm (blue) and 0.63 – 0.69 μm (red) (Figure 3-1). The relatively lower absorption (and high reflectance) of green wavelength light causes healthy vegetation to appear green to our eyes.

Additional pigments present in the leaf are yellow carotenes and pale yellow xanthophylls, with strong absorption in the blue wavelength region (0.4 – 0.5 μm). Phycoerythrin pigments absorb green and reflect both blue and red light. Usually, the chlorophyll masks these other pigments. However, when a plant undergoes senescence in

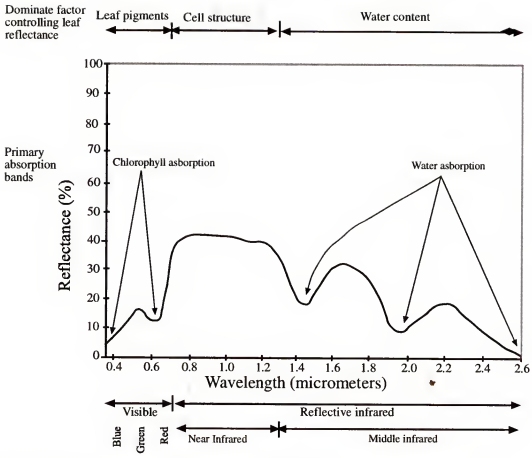

Figure 3-1. Spectral reflectance profile for healthy green vegetation (modified from Jensen, 1983).

the fall or encounters stress, the chlorophyll pigments decrease, allowing the other pigments to become dominant.

Chlorophyll absorption is a fundamental biophysical variable, and remote sensing data can be used as input to biogeographical and ecological studies. The absorption properties of canopies may be combined with other data, collected both *in situ* and by remote sensing methods to identify vegetation stress, yield, biomass, and other ecological variables.

Reflectance increases in the near-infrared region from 0.7 – 1.2 μm, where healthy green vegetation is characterized by high reflectance (40 – 50 percent), high transmittance (40 – 50 percent) through the leaf onto underlying leaves or ground, and low absorbance (Figure 3-2). This pattern is called the principle of leaf additive reflectance and explains that the greater the number of leaves in a healthy, mature canopy, the greater the near-infrared reflectance. Conversely, if the canopy is composed of only a single, sparse leaf layer then the near-infrared reflectance will not be as great because the energy that is transmitted though the leaf layer may be absorbed by the ground cover beneath (Verbyla, 1995; Campbell, 1996). Modeling these reflectance properties allows for estimates of LAI to be made using remote sensing data.

Another parameter of plant growth measured by remote sensing systems is water. A leaf contains water that is absorbed by the plant's roots and transported to the leaves via the plant's vascular system. If a leaf contains as much water as it can hold, it is said to be fully turgid, and much of the water is found in the spongy mesophyll portion of the plant. If a plant is not fully turgid, the ratio of water that it does contain to what it could contain is its relative turgidity. Liquid water exhibits five absorption bands in the visible

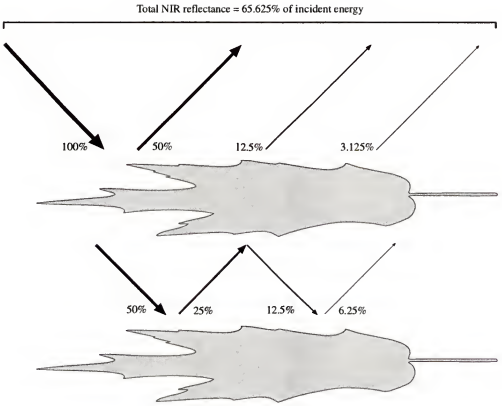

Figure 3-2. Principle of leaf additive NIR reflectance of two leaves assuming 50% reflectance and 50% transmittance

.

through middle infrared portion of the electromagnetic spectrum at 0.97, 1.19, 1.45, 1.94, and 2.7 μm (Figure 3-1). A particularly strong relationship exists between the reflectance in the middle-infrared region from 1.3 to 2.5 μm and the amount of water present in the leaves of a plant canopy. Water is a good absorber of middle-infrared energy, so the greater the relative turgidity of the leaves, the lower the middle-infrared reflectance. Conversely, as the moisture content of leaves decreases, reflectance in the middle infrared region increases substantially. As the amount of water in the intercellular air spaces decreases, incident middle-infrared energy is more intensely scattered at the interface of the intercellular walls resulting in greater middle-infrared reflectance from the leaf. This is one of the reasons that the Landsat Thematic Mapper(TM) was designed to be sensitive to two bands in this region (Jensen, 2000).

Much of the water in a plant is lost via transpiration that occurs through the stomata. Transpiration performs several important functions, including cooling the inside of the leaf because the escaping water vapor contains latent heat from evapotranspiration; maintaining water flow from the roots, through the stem, to the leaves; and ensuring a steady supply of dissolved minerals from the soil. As molecules of water vapor are lost to transpiration, the entire column of water is pulled upward. Plants can lose a considerable amount of water through transpiration each day. Thus monitoring the moisture content of plant canopies and correlating it with rates of transpiration can provide valuable information on the vegetation health (Campbell, 1996; Jensen, 2000).

Based on spectral characteristics, numerous studies have been conducted using remote sensing data to classify vegetation. These studies have ranged from forest type classifications (Roy, Ranganath, Diwakar, Vohra, Bhan, Singh, and Pandian., 1991;

Nelson, Horning, and Stone, 1987; Westman, Strong, and Wilcox, 1989; Nezry, Mougin, Lopes, Gastellu-Etchegorry, 1993) to other more detailed land cover classifications that relate land cover change to other processes such as carbon release (Murdiyarso and Wasrin, 1995). The spectral properties have also allowed for studies to be done that relate land cover change and carbon dynamics. For example, Woodcock, Collins, Gopal, Jakabhazy, Li, Macomber, Ryherd, Harward, Levitan, Wu, and Warbington (1994) estimated mean tree size and forest cover using a canopy reflectance model developed by Li and Strahler (1985; 1992). Woodcock et al. (1994) demonstrated that forest type and volume can be accurately mapped using remote sensing data, and measured conifer timber volume, which ranged from 80 to 459 m^3 / ha, in the Tahoe National Forest.

Leaf Area Index

Leaf area index (LAI) has been identified as the single most important variable for characterizing vegetation energy exchange for regional scale research (Running, Peterson, Spanner, and Teuber, 1986), and is defined the leaf area per unit ground area (Gower and Norman, 1991; Lymburner et al., 2000). LAI is useful in ecosystem analysis because of the importance of canopy structure in gas, water, C, and energy exchange with the atmosphere (Gholz, Curran, Kupiec, and Smith, 1997; Gower and Norman, 1991; Fassnacht et al., 1997; Herwitz, Peterson, and Eastman, 1990). In addition, canopy light interception, net photosynthesis, net primary production, stemwood production, and volume growth are directly proportional to LAI (Pierce and Running, 1998; Gholz, 1982). Because LAI is directly related to canopy-atmosphere dynamics, accurate

assessment of regional LAI is necessary to measure the magnitude of worldwide CO_2 flux and is useful to global climate change research (Fassnacht, 1997).

Traditional *in situ* measurement of LAI is labor intensive because obtaining many measurements over large geographic areas is difficult (Fassnacht et al., 1997). Traditional *in situ* measurement of LAI usually requires destructive harvesting of leaves within a vertical quadrat through the entire canopy or through leaf litterfall collection techniques. These direct methods are similar in that they require many replicates to account for spatial variability in the canopy and are time intensive and expensive (Green et al., 1997). However, these LAI measurements are accurate at a very specific geographic location, unambiguous, and well understood by ecologists.

Recently, new *in situ* unobtrusive methods have been developed to estimate LAI. One of these new methods is based on gap-fraction analysis. Gap fraction theory states that for whole canopies, the decrease in light intensity (light attenuation) with increasing depth can be described by the equation

$$IL / IO = e^{-kLAI(L)}$$

where *IL/IO* is the percentage of incident light at the top of the canopy (*IO*) reaching depth *L* in the canopy, *LAI*(*L*) is the cumulative LAI from the top of the canopy to point *L*, *k* is a stand or species specific constant, and *e* is the base of natural logarithms (Larcher, 1975; Aber and Melillo, 1991). Different types of vegetation have different *k* values, causing different rates of light attenuation for the same amount of leaf area. The principal factor causing this is differences in the angle at which the leaves are displayed (Larcher, 1975).

LAI measured using gap-fraction analysis assumes that leaf area can be calculated from canopy transmittance of light (the fraction of direct solar energy that penetrates the canopy). Gap-fraction techniques have been used to study LAI in many forest studies (e.g., Pierce and Running, 1988; Chason, Baldocchi, and Huston, 1991; Ellsworth and Reich, 1993; Nel and Wessman, 1993; Green et al., 1997).

To lessen the burden of making LAI *in situ* measurements, remote sensing data collection and analysis techniques represent a potential mechanism to estimate LAI over large geographic areas (Curran, Dungan, and Gholz, 1992; Running, Nemani, Peterson, Band, Potts, Pierce, and Spanner, 1989). These methods are based on the spectral properties of forests as described above.

Vegetation Indices

The basic principles of vegetation remote sensing described previously have allowed for the computation of various Vegetation Indices (VIs). These radiometric measures have been used to model LAI, absorbed photosynthetically active radiation (APAR), and the relative abundance and activity of green vegetation (Jensen, 2000; Lymburner et al., 2000; Liu and Huete, 1995). According to Running, Justice, Solomonson, Hall, Barker, Kaufmann, Strahler, Huete, Muller, Vanderbilt, Man, Teillet, and Carneggie (1994) a VI should have at least four properties:

1. maximize sensitivity to vegetative biophysical parameters;
2. normalize external effects (Sun angle, viewing angle, atmospheric anomalies);
3. normalize internal effects (topography, soil variations, nonphotosynthetic components); and,

4. be coupled to some specific measurable parameter such as LAI or biomass.

VIs range from simple near-infared (NIR) to red (R) spectral reflectance ratios to complex linear band equations that account for atmospheric and biophysical influence (for example, the Soil Adjusted Vegetation Index (Huete, Liu, Batchil, and van Leeuwen, 1997)). The ratio of reflected radiance from the NIR and red bands incorporates a significant amount of illumination and topographic variation, and forms a stable indicator of the vigor of green vegetation (Liu and Huete, 1995).

One of the most important vegetation indices is the Normalized Difference Vegetation Index (NDVI). It has been identified as a useful tool to examine regional, continental, and global photosynthesis (Bonan, 1993; Running et al., 1994). The NDVI is calculated using the equation (Rouse, Haas, Schell, and Deering, 1974):

$$NDVI = \frac{NIR - RED}{NIR + RED}$$

NDVI has been used in phenological studies, in land-cover classification, in global climate change models, and even to predict outbreaks of insect-borne diseases (Justice, Townshend, Holder, and Tucker, 1985, Sellers, Tucker, and Collatz, 1994). NDVI has been correlated with biophysical plant canopy properties (Pinty, Leprieur, Verstraete, 1993), including its relation to biomass (Pearson and Miller, 1972; Tucker, 1979; Elvridge and Lyon, 1985; Box, Holben, and Kalb, 1989), LAI (Holben, Tucker, and Fan, 1980; Badhwar, MacDonald, Hall, and Carnes, 1986; Clevers, 1988; 1989; Spanner, Pierce, Peterson, and Running, 1990; Gholz et al, 1997; Chen, 1996) primary productivity (Tucker and Sellers, 1986), photosynthetic radiation (Asrar, Fuchs,

Kanemasu, and Hatfield, 1984; Choudhury, 1987; Chen 1996), and other ecological parameters (Cihlar, St-Laurent, and Dyer, 1991).

Unfortunately, some studies have found that the empirically derived NDVI may be unstable and vary with changing environmental conditions such as soil types and plant water content (Huete et al., 1997). Because of this, several modified versions of NDVI have been developed to reduce the sensitivity of NDVI to varying substrates (e.g., soil and water) (Lawrence and Ripple, 1998).

For example, the Soil Adjusted Vegetation Index (SAVI) introduces a soil adjustment factor, *L*, which is based on the amount of vegetation, subjectively chosen from 0 (for high vegetation) to 1 (for low vegetation) into the NDVI equation to minimize soil background influences (Huete, Hua, Qi, Chehbouni, and van Leeuwen., 1992; 1997). In the absence of explicit knowledge of the vegetation cover, an *L* value of 0.5 has been suggested and generally applied (Lawrence and Ripple, 1998):

$$SAVI = \frac{NIR - RED}{NIR + RED + L}$$

In this study, the simple ratio (SR) and the SAVI were used in conjunction with NDVI. The SR is the near infrared to red ratio (NIR/Red), and was first developed by Birthe and McVey (1968).

Each of the preceding VIs are known collectively as "ratio-based" VIs. In contrast, Kauth and Thomas (1976) used the technique of sequential orthogonalization to calculate a transformation of the original Landsat Multispectral Scanner (MSS) remote sensor data. They called it the "Tasseled Cap" transformation because of its appearance as a tasseled cap in feature space. They named the four new axes the soil brightness

index, green vegetation index, yellow stuff index, and non-such index. These names indicate the characteristics that each measures. Crist (1985) derived global coefficients for each of the tasseled cap axes using TM remote sensor data. However, Huete, Post, and Jackson (1984) and Ezra, Tinney, and Jackson (1984) provide insight into the importance of calculating site-specific coefficients, rather than using global coefficients. In this study, site-specific "Tasseled Cap" coefficients were determined as explained by Jackson (1983) (Appendix A).

LAI and Remote Sensing Vegetation Indices

Several VIs have been created to study different stages of plant growth and allow for the rapid estimation of some biophysical variables. For example, LAI can be estimated with TM data and correlated with vegetation indices such as NDVI (Jensen, 2000; Liu and Huete, 1995; Lymburner et al., 2000). Herwitz et al. (1990) concluded that a simple NIR / Red ratio correlated positively with LAI of various pine plantations in central Massachusetts, and that changes (thinned and unthinned canopies) in canopy LAI can be detected using TM data. Carlson and Ripley (1997) concluded that LAI and NDVI are correlated and that NDVI can be indicative of LAI values. Chen and Cihlar (1996) found that the simple NIR / Red ratio and NDVI are correlated with LAI (up to $r^2 = 0.52$). Fassnacht et al. (1997) studied LAI using a variety of statistical methods. They concluded that multivariable regression approaches were the most accurate to estimate LAI in the forests of Wisconsin. In one study, green vegetation in the Mount St. Helens, Washington area was compared using a variety of regression techniques with vegetation indices (Lawrence and Ripple, 1998). The authors found that the most accurate

representation of green vegetation was stepwise regression combining six Thematic Mapper bands. Green et al. (1997) analyzed the LAI of mangrove forests in the Nile Delta using NDVI. They concluded that NDVI was an accurate indicator of LAI in mangrove ecosystems. Another study (Weiss and Baret, 1999) estimated biophysical variables including LAI using the relatively coarse resolution (1.15 x 1.15 km) SPOT4/Vegetation radiometer based on a synthetic data set with several digital image processing techniques. They concluded that high levels of heterogeneity in pixels could affect biophysical variables such as LAI.

Despite the apparent utility of NDVI and LAI, some studies have found a threshold LAI value of 2 - 4 where NDVI fails to increase in relation to increased LAI values (Figure 1-1). LAI saturates because solar radiation reflected from underlying ground and leaf levels is largely attenuated by the dense overstory (Carlson and Ripley, 1997). In addition, variations in soil brightness can produce large variations in NDVI from one scene to the next (Carlson and Ripley, 1997; Datt, 1998). Lawrence and Ripple (1998) also showed that vegetation indices such as the NDVI or SAVI unnecessarily restrict regression analysis because ratio-based VIs are unable to model both the red and NIR reflectances separately.

Artificial Neural Networks

Quantitative biophysical information has been extracted from remote sensing imagery for the last three decades. The data obtained from processed remote sensing images have usually incorporated univariate and multivariate statistical methods that are now well known to remote sensing scientists (Benediktsson, Swain, and Ersoy, 1990;

Jensen, 1996). In recent years, there has been a growing interest in Artificial Neural Networks (ANNs). ANN techniques have been applied to computer science, artificial intelligence, pattern recognition and identification, and biomedical engineering (Jin and Liu, 1997). ANNs represent a different approach to analyzing remotely sensed imagery because they do not rely on statistical relationships, do not require normally distributed input data, and they are able to estimate continuous functions from data without specifying mathematically how outputs depend on inputs (Gopal and Woodcock, 1996). ANNs have been used in remote sensing applications to classify images (Bischof, Schneider, and Pinz, 1992), extract biophysical characteristics (Jensen and Qui, 2000), and incorporate multisource data (Benediktsson et al, 1990).

ANNs grew out of research in artificial intelligence, specifically attempts to mimic the fault-tolerance and capacity to learn of biological neural systems by modeling the low level structure of the brain (Haykin, 1994). Work on ANNs has been motivated from its inception by the recognition that the brain computes in a very different way than digital computers (Haykin, 1994).

A neuron is the fundamental processing unit of an ANN. Neurons are analogous to the human brain's biological neurons. Typically, biological neurons are five to six orders slower than silicon logic gates, but the brain makes up for the slow rate by having a very large number of neurons with massive interconnections between them. It is estimated that there are on the order of 10 billion neurons in the human cortex, and 60 trillion connections among them (Haykin, 1994). The brain is a highly complex, nonlinear, parallel computer (information-processing system) that has the capacity to organize neurons to perform certain computations (e.g., pattern recognition, perception,

and motor control) faster than the fastest computers in existence today. Artificial neural networks are "massively parallel distributed processors that have a natural propensity for storing experimental knowledge and making it available for use" (Haykin, 1994). They resemble the brain in two respects: 1. knowledge is acquired by the network through a learning process; and, 2. interneuron connection strengths known as synaptic weights are used to store the knowledge (Haykin, 1994).

A particular type of ANN, multilayer perceptron networks, were used in this study. These networks have the following distinctive characteristics (Haykin, 1994):

1. The network contains one or more hidden layers that are not a part of the output or input of the network. These hidden neurons enable the network to learn complex tasks by extracting progressively more meaningful features from the inputs.

2. The network has a high degree of connectivity that is determined by the synapses of the network.

ANNs have applications in the fields of classification, pattern recognition, and signal processing (Keiner and Yan, 1998). ANNs represent a different approach to problems such as pattern recognition because they do not rely on statistical relationships. Rather, ANNs adaptively estimate continuous functions from data without mathematically describing how outputs depend on inputs (e.g., adaptive model-free function estimation using a nonalgorithmic[2] strategy) (Gopal and Woodcock, 1996). Therefore, ANNs are capable of modelling any complex system (Jensen and Qui, 2000).

In summary, the use of ANNs offers the following useful capabilities (Haykin, 1994):

[2] Nonalgorithmic strategies are those that do not have a clear path at the beginning of a task. The path to a solution is not discernible from a single vantage or starting point; multiple solutions are possible.

1. Nonlinearity. A neuron is a nonlinear device, thus making the network nonlinear. This characteristic is especially important if the phenomena being measured are nonlinear.

2. Input-Output Mapping. Often referred to as supervised learning, this allows the modification of synaptic weights of ANNs by applying a set of training samples.

3. Adaptivity. ANNs have the ability to adapt their synaptic weights to changes in the environment.

4. Evidential Response. ANNs can be designed to provide not only information about which values to select, but also provide confidence in the decision made.

5. Contextual Information. Every neuron in the network is potentially affected by the global activity of all other neurons in the network. Consequently, contextual information is dealt with easily.

6. Uniformity of Analysis and Design. Neurons, in one form or another, represent a component common to all ANNs. This commonality makes it possible to share theories and learning algorithms in different applications of ANNs.

Network Architecture

A typical neural network consists of three or more interconnected layers or nodes: one input layer, one output layer, and one or more hidden layers. Nodes in subsequent layers are called neurons because of their neuron-like functions. Each neuron consists of two parts, a linear summation function and a nonlinear activation function. The inputs to each neuron are first routed through the summation function (Keiner and Yan, 1998). The output of this function inside the neuron at node j is given by the following equation:

$$y_j = \sum_{i=1}^{n} w_{ij} x_i + b_j$$

where x_i are the inputs, w_{ij} are the weights associated with each input/node connection, and b_j is the bias associated with node j. The inputs to the neuron are multiplied by their associated weights, summed, and added to the bias.

Each input node in this research corresponded to a Landsat Thematic Mapper brightness value. The input layer values were distributed to nodes in the hidden layers, where the summation and activation functions were implemented. The output values of the hidden layer then become the input values of the network's output layer that also performs the summation and activation functions. The output of this layer is the LAI value shown in the following equation (Keiner and Yan, 1998):

$$LAI = ag(\sum_{k=1}^{j} w_k z_k + \beta)$$

For the output layer, w_k are the weights between the hidden layer and the output layer, β is the bias associated with the output layer, and j is the number of nodes in the hidden layer. The output is scaled by a factor, a that is determined in the training phase. a depends on the range of the output parameter and is set during network training. β is also set determined during network training (Keiner and Yan, 1998). G is a squashing function that limits the permissible amplitude range of the output signal to some finite value. The normalized range of the output of a neuron is between –1 and 1 (Haykin, 1994).

The number of hidden layers needed depends on the complexity of the function to be represented. Generally speaking, the network needs enough nodes to model the function correctly, but too many nodes can result in increased training time and possibly

overfit the function. Overfitting occurs where the network not only learns the correct pattern, but also incorporates noise in the inputs, which results in poor outputs when real data are applied to the network. Before training, the weights associated with each connection are randomly generated to "seed" the calculations.

Network Training

The purpose of a neural network is to determine the correct output (e.g., an accurate LAI estimate) when an input pattern (e.g., remote sensing brightness values) is given. To do this, the network learns by training example data. The procedure to perform the learning process is called a learning algorithm, the function of which is to modify the synaptic weights of the network to attain a desired design objective (Haykin, 1994). This is possible by providing the input layer and the training data (output layer), and is done by comparing the current activation of neurons in the output layer to a desired output response. The difference is used to weight neurons throughout the network. For this study, the input layer was reflectance data from each of the spectral bands. Learning achieves a set of weights that will produce an output most resembling the target that ultimately determines the behavior of the network (Jensen and Qui, 2000; Keiner and Yan, 1998).

The internal weights must be changed to correct network errors and modify the network output. This is accomplished through a learning algorithm called back-propagation. Back-propagation networks were developed by Werbos (1974) and Rumelhart, Hinton, and Williams (1986) to improve the efficiency of multilayer network training. Back-propagation allows the network to adjust its weights, starting with the

output layer and working back through the network (Keiner and Yan, 1998; Haykin, 1994). Specifically, the back-propagation process consists of two passes through the different layers of a network: a forward pass and a backward pass. In the forward pass, an input vector is applied to the sensory nodes of the network, and its effects are propagated layer by layer through the network. During this pass the synaptic weights are all adjusted. During the backward pass, the synaptic weights are all adjusted such that the sum-squared error (SSE) is minimized. The SSE equation follows:

$$SSE = \frac{1}{2} \sum_{i=1}^{n} (t_i - o_i)^2$$

where the output o is compared with known correct output t. The difference between o and t is the network error.

The Widrow-Huff rule calculates the incremental change in the network's weights based on which direction of change will decrease the SSE. The derivative of the SSE with respect to the weight w_{ij} (the weight at node j receiving input from node i) is given by the following equation (Keiner and Yan, 1998):

$$\frac{SSE}{w_{ij}} = -\sigma_j o_i$$

where σ_i is a change factor for the weight, w_{ij} with input o_i from the previous layer. The weight is then modified as follows (Keiner and Yan, 1998):

$$w_{ij}(t+1) = w_{ij}(t) + \eta \sigma_j o_i$$

where η is a learning rate term and t is the time step or the next iteration. This training process operates by repeatedly using the data in the training sets to change the weights until an acceptable error level is reached (Keiner and Yan, 1998). The learning rate η changes during training to accelerate towards a solution in the beginning then slows as a solution gets closer to avoid overshooting the solution (Keiner and Yan, 1998).

Neural Networks and Remote Sensing

ANN classifiers have been successfully used with remote sensing data because they take advantage of the ability to incorporate non-normally distributed numerical and categorical GIS data and image spatial information (Jensen and Qui, 2000). ANN classifiers usually outperform conventional remote sensing classifiers (e.g., parallel-piped, maximum likelihood) because of their lack of assumptions about normality in the datasets, the considerable ease in using multidimensional datasets, and the efficacy in capturing some of the inherent nonlinearity in such data (Gopal and Woodcock, 1996; Jensen and Qui, 2000).

Several studies have demonstrated the utility of employing ANNs with remote sensing data. Jensen and Qui (1999) used an ANN to discriminate conifer stand age in southern Brazil. The authors found that ANNs were able to model complex nonlinearity of biophysical processes and ANNs were better at extracting conifer stand age than traditional image processing techniques. In addition, Jensen and Qui (1999) concluded that ANNs are ideal for modeling the latent complexity of plant biophysical characteristics during the plant life cycle using remotely sensed spectral data. They also concluded that ANN analysis techniques have potential for more accurately modeling

biophysical forest parameters than do traditional statistical techniques. This is one of the few studies that has used ANNs to estimate biophysical characteristics of forests.

Weiss and Baret (1999) used ANNs to measure biophysical variables such as photosynthetically active radiation and LAI from the International Satellite Land Surface Climatology Project (ISLSCP) (Sellers et al., 1994; Sellers, Los, and Tucker, 1995). They concluded that biophysical variables predicted from ANNs appear to be more accurate than those using the NDVI-based methods. Gopal and Woodcock (1996) used ANNs and remote sensing to detect conifer forest change after a long drought in the Lake Tahoe Basin in California. They determined that ANNs are able to monitor conifer mortality more accurately than normal remote sensing change detection algorithms. Bischof et al. (1992) classified Landsat TM data on a pixel-by-pixel basis. They found that ANN classification is more accurate than Gaussian maximum likelihood classification and went further to use an ANN for post-classification smoothing. Other studies have also been done that use ANNs for land cover mapping and have had accuracy rates that range from 85 to 95% (Yoshida and Omatu, 1994; Benediktsson et al., 1990; Gopal, Woodcock, and Strahler, 1999). Chlorophyll and suspended sediments in water can be more accurately predicted using ANNs than with traditional regression techniques (Keiner and Yan, 1998).

Satellite Imagery

Remote sensing is performed using an instrument often referred to as a remote sensor (Jensen, 2000). The remote sensor used in this study was the Landsat 5 Thematic Mapper (TM). Landsat 5 TM was launched on 1 March 1984 and was built, as the name

implies, for the identification and classification of landscape land uses and patterns (Aber and Melillo, 1991; Jensen, 2000). Whereas previous remote sensing systems recorded energy in bands determined to be most useful for general vegetation and geology studies (e.g., Landsat Multispectral Scanner), the Landsat TM bands were selected after years of analysis for their value in measuring water penetration, discrimination of vegetation type and vigor, plant and soil moisture measurement, and other applications. The TM bands were selected to make use of the dominant factors controlling leaf reflectance, such as leaf pigmentation, leaf and canopy structure, and moisture content as described above (Jensen, 2000; Figure 3-1).

Landsat image paths are based on a world reference system (WRS). The WRS has 233 paths from east to west and rows that correspond to degrees latitude. The scenes used in this study are 17-39, 16-39, and 16-40 (Lillesand and Kiefer, 2000). Historical TM data are available for public purchase from Space Imaging, Inc. (http://www.spaceimaging.com/) and the EROS Data Center of the U.S. Geological Survey (http://edcwww.cr.usgs.gov/). Current Landsat 7 data are available from the U.S.G.S.

CHAPTER 4
METHODS

Goals

The goal of this research was to develop improved methods of estimating landscape-scale LAI from satellite remote sensing data, and apply these methods to two ecological studies. This study compared the accuracy of LAI estimates made by digital image processing, ANNs, and statistical techniques.

Hypotheses

The theory of light behavior in forest canopies is explained by absorbance and reflectance properties of leaf, branch, stem, soil surfaces, and photosynthetic pigments and water in the leaf cell structure. The detailed theory has already been described in chapter three, but it will be summarized in this section as part of hypothesis development.

H_1: LAI and VIs are correlated, and simple regression can estimate LAI.

The first hypothesis will test the effectiveness of simple linear regression between LAI (dependent variable) and VIs (independent variables) to predict LAI. It depends on known relationships between healthy vegetation, red energy absorption, and near-infrared energy reflectance (Datt, 1998).

H_2: Multiple regression using data from each of the six Landsat TM bands as independent variables is more accurate than simple regression to estimate LAI.

The second hypothesis addresses the possibility that the use of vegetation indices and simple linear regression may unnecessarily constrain LAI estimates because any function performed using vegetation indices is unable to treat both bands (red and near infrared) simultaneously. Thus, models using vegetation indices are not able to treat individual red and near infrared responses independently. For example, if the red response is curvilinear, and the near infrared response is not, a compromise fit is necessary (Lawrence and Ripple, 1998). At least one study (Ripple, 1994) has found that regression of LAI on individual bands explains more variability than regression against NDVI alone.

H_3: ANNs trained using data from each of the six reflectance bands as input variables is more accurate than any of the regression methods for estimating LAI

In some studies (e.g., Hepner, Logan, Ritter, and Bryant, 1989; Jensen and Qui, 2000; Weiss and Baret, 1999), ANNs accurately modeled biophysical variables, and outperformed conventional statistical techniques. This is because ANNs adaptively estimate continuous functions from data without mathematically describing how outputs depend on inputs, ANNs do not rely on linear relationships, ANNs are capable of modeling any complex data, and ANNs have been shown to be more accurate than statistical techniques (Gopal and Woodcock, 1996; Jensen and Qui, 2000).

H_4: The techniques developed in this research can be applied to ecological studies.

Much interest exists in the questions posed by regional-scale LAI dynamics, and the new methods developed here allow scientists to study them. One case study will look

at the effects of fire suppression on sandhill ecosystem LAI, and the other will examine the difference in LAI in two central Florida urban forests.

Methods

Field LAI Measurements.

LAI was measured by using the gap-fraction method with a Decagon AccuPar Ceptometer™. The ceptometer consists of a linear array of 80 adjacent 1 cm^2 photosynthetically active radiation (PAR) sensors along a bar. LAI calculated with the ceptometer has been found to have r values of 0.97 when compared to destructive LAI measurements (Pierce and Running, 1988).

LAI is a function of canopy transmittance, the fraction of direct solar radiation that penetrates the canopy (Green et al., 1997). Solving for LAI in the gap fraction analysis equation in Chapter 3 yields the following where incident sunlight outside of the canopy, Q_1, and the amount of direct solar energy incident to the ceptometer, Q_2, when it is held below the canopy are used to compute LAI:

$$LAI = \frac{-\ln \frac{Q_1}{Q_2}}{k}$$

and k is a species dependent light extinction coefficient that incorporates the zenith angle of the sun and leaf angle of inclination into the calculation (Decagon, 1994; Smith, Sampson, and Long, 1991; Gholz, 1991).

North-south and east-west PAR measurements were made on each corner of a north-oriented 20 x 20 m quadrat and averaged for input to the LAI equation in 64

random locations throughout the study area. A Global Positioning System (GPS) location was measured in the Universal Transverse Mercator (UTM) coordinate system in the middle of each quadrat for input into a GIS.

Brightness Value Extraction

Remote sensing brightness values (BVs) for each of the six Landsat TM bands were extracted from the imagery at each sample site on a pixel-by-pixel basis. BVs are the average reflectances for each 28.5 x 28.5 m pixel area for each band in different portions of the electromagnetic spectrum. The GPS locations were used to extract interpolated BVs from TM bands 1-5, and 7 using a GIS program written in the ArcView Avenue scripting language (Appendix B).

Multiple Regression of LAI and Six TM Spectral Bands.

The brightness values were then used with the *in situ* LAI measurements to estimate LAI based on the relationship between forest canopy reflectance and six TM bands. Correlation and regression analyses are common methods used to model forest characteristics with remotely sensed data, and a well-formulated model can be used to predict the same characteristics at new locations (Jensen and Qui, 2000).

Multiple regression was performed using BVs from the six TM bands as the independent variables and *in situ* LAI as the dependent variable. This yielded a regression function that was applied to the BVs from other areas to estimate LAI.

Vegetation Indices and LAI

Vegetation indices were calculated from the brightness values using the equations presented in Chapter 3. NDVI and SAVI values ranged from 0.16 to 0.70 with those values closest to 1 representing the most 'green' areas. SR values ranged from 1.38 to 5.58, where the higher values denote greener pixels. GVI values ranged from –91.35 to 15.02, with the higher values also representing greener pixels. *In situ* LAI values were linearly regressed with each VI that yielded regression functions for each VI. These regression functions were then used to estimate LAI in other areas.

Artificial Neural Networks and LAI

An ANN was created and trained using TM bands 1-5 and 7 as inputs, and *in situ* LAI as the output. ANNs can be trained using remote sensor data from image areas that are known and then applied to other image areas (e.g., Gopal and Woodcock, 1996; Bischof et al., 1992). The network was trained with different numbers of hidden neurons. The network architecture with the lowest network error value was determined to be the most accurate to estimate LAI. The network was then applied to other image areas.

Overall Accuracy

Each method's estimate was then analyzed to determine the most accurate way to measure LAI using remote sensing data. Thirty LAI *in situ* verification points were measured throughout the study area. These points were measured in exactly the same way as the 64 *in situ* LAI points used to create the models. The brightness values and vegetation indices of each verification point were input into each LAI estimation model.

The estimated LAI values were then compared with the *in situ* LAI values using the root mean square error (RMSE), and graphed in X,Y scatter plots to examine the distribution of the data. Those measurements with the smallest RMSE were assumed to be the most accurate. RMSE is a measure of the deviation of the predicted values (LAI derived using various techniques) from the actual values (*in situ* LAI measurements). The RMSE equation follows: (Miller and Kahn, 1962; Verbyla, 1995; Jensen, 1996; Manly, 1992).

$$RMSE = \sqrt{\frac{\sum_{x=1}^{n} (X_{pred} - X_{actual})^2}{n}}$$

The method with the smallest RMSE was then used in two LAI ecological studies.

CHAPTER 5
RESULTS

Regression Analyses

The 64 training measurements were made in locations throughout the study area and are summarized in Table 5-1(mean LAI = 3.03; s.d. = 2.19; maximum = 6.94; minimum = 0.0). The multiple regression function determined using six bands is ($F = 47.0$; $R^2 = 0.832$):

$$LAI = -9.93 + 0.212 * Band1 - 0.222 * Band2 + 0.115 * Band3 + 0.101 * Band4 - 0.0701 * Band5 - 0.0450 * Band7$$

The *F*-test for the model and the *t*-test for slope were both significant at $p < 0.001$ indicating that multiple band regression may be used to estimate LAI values. When the brightness values of the 30 verification points were input into this regression equation to estimate LAI, and these values were compared with the *in situ* LAI values, an RMSE of 0.837 resulted.

Figure 5-1 shows the graph of *in situ* LAI values (X) and LAI values estimated from all band regression (Y). In the graph, there seems to be a clustering of points below *in situ* LAI values of 3.0 and a cluster of LAI points above 3.0. Upon further investigation, the RMS errors of the six band regression estimator of *in situ* LAI values less than 3.0 was 0.701, and 0.913 for those *in situ* LAI values greater than 3.0.

The brightness values obtained from the remote sensing imagery were used to calculate vegetation indices (VIs). NDVI and SAVI measured exactly the same (mean =

. Table 5-1. The 64 *in situ* LAI measurements and their associated Landsat Thematic Mapper brightness values and descriptive statistics.

Band 1	Band 2	Band 3	Band 4	Band 5	Band 7	Lai
74.2	28.0	30.2	67.1	95.0	35.2	1.4
72.2	28.0	28.1	78.7	81.1	29.1	5.2
67.0	24.0	18.0	90.9	54.5	13.3	6.4
67.1	24.6	18.2	95.9	58.0	14.6	5.1
67.0	24.0	19.0	82.9	56.7	16.0	2.5
75.0	29.9	31.9	68.1	101.2	40.2	0.8
67.5	24.3	19.4	84.2	56.9	15.7	4.1
71.6	28.3	27.6	78.2	84.6	31.2	2.1
69.3	26.3	22.6	66.2	61.2	19.2	4.0
67.0	25.0	21.0	80.1	59.3	17.3	4.1
66.5	25.0	18.4	83.8	50.5	13.4	3.9
68.5	25.5	20.6	78.9	48.9	13.5	6.0
67.5	26.1	19.3	93.6	57.2	14.2	6.9
67.9	26.4	20.8	85.4	58.1	16.6	5.0
69.0	26.0	22.2	76.1	61.1	18.0	4.9
68.0	25.1	18.6	99.8	56.1	14.4	6.9
66.0	24.0	18.0	97.2	55.6	14.6	6.9
73.7	28.0	30.9	67.1	82.3	30.6	1.2
85.1	35.4	45.3	66.8	134.9	65.1	0.0
74.0	28.0	32.0	61.0	84.0	33.0	1.3
75.8	29.5	34.2	62.8	99.4	41.1	1.3
71.4	27.9	30.2	65.7	85.4	33.2	1.6
76.5	30.4	34.5	62.8	102.1	42.6	1.5
76.3	29.1	32.1	63.9	89.7	35.7	3.7
72.5	27.5	31.5	61.2	89.0	33.7	2.0
70.9	26.7	29.0	64.0	82.1	29.9	2.4
76.1	29.7	33.7	58.9	98.8	41.7	0.0
74.0	28.0	33.0	61.0	84.3	32.9	2.8
73.3	28.8	31.1	77.5	84.8	31.7	3.3
77.7	30.9	34.8	69.0	108.3	44.8	0.0
79.4	32.1	39.3	65.8	115.9	49.7	0.9
70.3	27.2	28.1	67.3	74.5	28.1	0.9
76.7	29.6	31.1	62.3	78.9	31.7	2.3
75.9	29.2	33.5	56.6	99.0	41.1	0.3
87.0	37.4	48.0	72.8	123.9	55.7	0.7
75.6	28.2	30.4	65.7	96.9	37.7	1.4
73.8	28.2	29.0	78.1	83.9	30.8	5.2
66.9	24.2	18.9	88.1	54.4	13.3	6.4
68.0	25.0	17.7	98.7	58.3	13.8	5.1
76.0	30.9	33.0	66.9	106.7	42.9	0.8
68.8	24.2	19.3	86.7	56.4	15.9	4.1
71.2	29.0	27.0	82.1	79.6	28.3	2.1
69.8	26.3	23.7	64.2	59.8	20.0	4.0
65.8	25.0	21.0	77.2	59.3	18.0	4.1
66.8	26.2	18.7	87.8	52.9	13.9	3.9
68.6	25.6	21.1	83.2	50.6	14.7	6.0
68.0	25.9	19.7	94.3	57.1	14.3	6.9

Table 5-1. Continued

	Band 1	Band 2	Band 3	Band 4	Band 5	Band 7	Lai
	69.3	27.7	21.6	89.8	62.1	18.4	5.0
	70.0	26.3	22.7	76.3	61.6	19.2	4.9
	68.4	25.5	18.2	101.0	57.1	14.4	6.9
	66.0	25.0	19.4	100.8	56.2	13.6	6.9
	74.2	28.4	31.5	68.0	83.9	29.9	1.2
	88.0	36.9	48.7	67.1	146.0	72.5	0.0
	75.7	29.0	33.0	61.9	88.9	35.6	1.3
	75.7	29.4	35.3	61.2	96.9	40.5	1.3
	72.3	28.1	30.2	66.1	83.7	32.5	1.6
	77.7	31.3	35.7	62.5	104.5	44.9	1.5
	72.7	28.0	31.9	60.3	90.2	34.3	2.0
	69.7	27.1	28.9	63.3	78.7	29.4	2.4
	76.8	30.3	32.7	57.9	100.4	41.9	0.0
	76.0	29.4	34.4	61.1	91.9	36.9	2.8
	71.8	28.7	28.9	82.0	77.1	27.1	3.3
	76.4	30.2	33.9	64.2	107.2	42.2	0.0
	62.0	23.0	22.5	47.5	49.5	17.0	0.8
Mean	72.2	27.8	27.7	74.0	79.1	28.9	3.0
Std. Dev	5.1	2.9	7.6	13.1	22.5	13.5	2.2

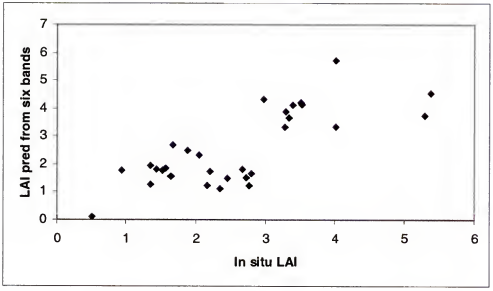

Figure 5-1. Scatter plot of predicted LAI and in situ LAI using six band regression

0.45, s.d. = .16). The VIs (SR, NDVI, SAVI, and GVI) were each linearly regressed against *in situ* LAI. Table 5-2 summarizes the vegetation indices for each of the 64 points. The regression functions derived from *in situ* LAI and remotely derived vegetation indices are:

$$LAI = -2.423 + 12.184 * NDVI$$

$$LAI = -2.420 + 12.236 * SAVI$$

$$LAI = -1.349 + 1.472 * SR$$

$$LAI = 4.815 + 0.072 * GVI$$

NDVI ($F = 201.89$, $p < 0.001$; $R^2 = 0.7651$), SAVI ($F = 202.12$, $p < 0.001$; $R^2 = 0.7653$), SR ($F = 186.57$, $p < 0.001$; $R^2 = 0.751$), and GVI ($F = 203.635$, $p < 0.001$; $R^2 = 0.767$) and *in situ* LAI were each significantly correlated with LAI. Figures 5-2, 5-3, 5-4, and 5-5 show the regression plots of each of the VIs and *in situ* LAI. Although the NDVI and LAI relationship didn't saturate, LAI at any given NDVI spans a very wide range of values. SAVI, SR, and GVI and LAI each have a similar pattern.

The 30 verification points (mean LAI = 2.60; s.d. = 1.17; maximum = 5.38; minimum = 0.5) were extracted from each of the three different types of ecosystems used to train the regression functions and the artificial neural networks. Table 5-3 summarizes the 30 verification points listing brightness and LAI values, and Table 5-4 shows the 30 points and corresponding VI values.

After comparing the *in situ* LAI values of the 30 verification points and the LAI estimates of each regression function, and graphing the estimated LAI values and *in situ* LAI values it became apparent that the same gap that was evident on the six band regression scatter plot was also present in the graphs of each of the ratio-based VI

Table 5-2. *In situ* LAI and associated remote sensing derived Vegetation Index (VI) values.

NDVI	SAVI	SR	GVI	Lai
0.38	0.38	2.22	-41.86	1.36
0.47	0.47	2.80	-23.03	5.17
0.67	0.67	5.05	9.50	6.37
0.68	0.68	5.28	10.34	5.09
0.63	0.62	4.36	1.63	2.46
0.36	0.36	2.13	-47.20	0.77
0.63	0.62	4.35	2.35	4.09
0.48	0.48	2.84	-25.88	2.13
0.49	0.49	2.93	-14.74	4.01
0.59	0.58	3.82	-2.69	4.11
0.64	0.64	4.54	6.91	3.88
0.59	0.58	3.84	3.71	6.00
0.66	0.66	4.85	9.02	6.92
0.61	0.61	4.11	1.73	5.03
0.55	0.55	3.42	-7.38	4.92
0.69	0.68	5.36	13.91	6.94
0.69	0.68	5.40	12.87	6.93
0.37	0.37	2.17	-32.93	1.19
0.19	0.19	1.47	-81.18	0.00
0.31	0.31	1.91	-39.20	1.28
0.30	0.29	1.84	-50.66	1.30
0.37	0.37	2.18	-36.05	1.60
0.29	0.29	1.82	-52.91	1.50
0.33	0.33	1.99	-41.98	3.73
0.32	0.32	1.94	-41.87	1.98
0.38	0.37	2.21	-33.73	2.37
0.27	0.27	1.75	-53.09	0.00
0.30	0.30	1.85	-39.49	2.78
0.43	0.43	2.49	-27.73	3.32
0.33	0.33	1.98	-53.35	0.00
0.25	0.25	1.67	-63.00	0.86
0.41	0.41	2.39	-26.25	0.91
0.33	0.33	2.00	-35.23	2.30
0.26	0.26	1.69	-54.45	0.30
0.20	0.20	1.52	-68.28	0.69
0.37	0.37	2.16	-45.10	1.36
0.46	0.46	2.69	-26.10	5.17
0.65	0.64	4.67	7.54	6.37
0.70	0.69	5.57	12.32	5.09
0.34	0.34	2.03	-52.53	0.77
0.64	0.63	4.49	4.01	4.09
0.51	0.50	3.04	-19.15	2.13
0.46	0.46	2.70	-15.89	4.01
0.57	0.57	3.68	-4.70	4.11
0.65	0.65	4.70	7.91	3.88
0.60	0.59	3.95	5.07	6.00
0.65	0.65	4.78	9.40	6.92

Table 5-2. Continued

	NDVI	SAVI	SR	GVI	Lai
	0.61	0.61	4.16	1.25	5.03
	0.54	0.54	3.37	-8.18	4.92
	0.70	0.69	5.56	14.14	6.94
	0.68	0.67	5.20	15.02	6.93
	0.37	0.36	2.16	-33.20	1.19
	0.16	0.16	1.38	-91.35	0.00
	0.30	0.30	1.87	-42.89	1.28
	0.27	0.27	1.74	-50.21	1.30
	0.37	0.37	2.19	-34.68	1.60
	0.27	0.27	1.75	-55.81	1.50
	0.31	0.31	1.89	-43.49	1.98
	0.37	0.37	2.19	-31.85	2.37
	0.28	0.28	1.77	-54.74	0.00
	0.28	0.28	1.77	-46.04	2.78
	0.48	0.48	2.84	-17.82	3.32
	0.31	0.31	1.89	-54.68	0.00
	0.36	0.35	2.11	-18.49	0.83
Mean	0.45	0.45	2.98	-24.88	3.03
St. Dev.	0.16	0.16	1.29	26.85	2.20

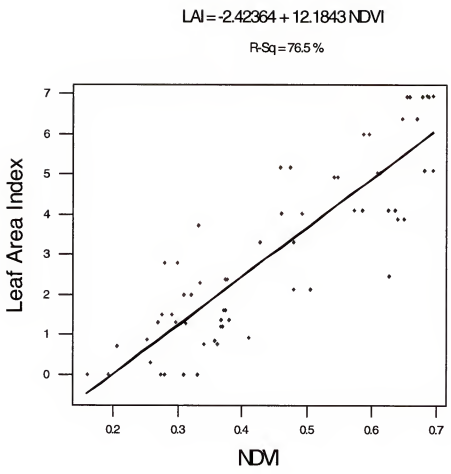

Figure 5-2. Regression plot and equation of NDVI and LAI.

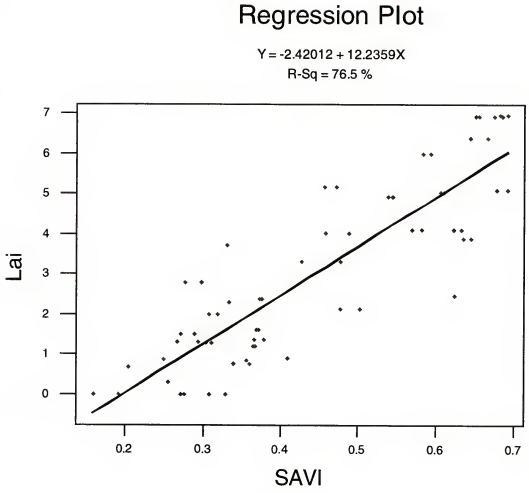

Figure 5-3. Regression plot of LAI and SAVI with equation.

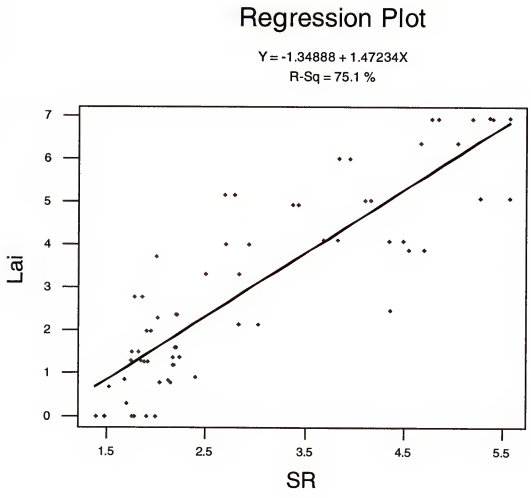

Figure 5-4. Regression plot of LAI and SR with equation.

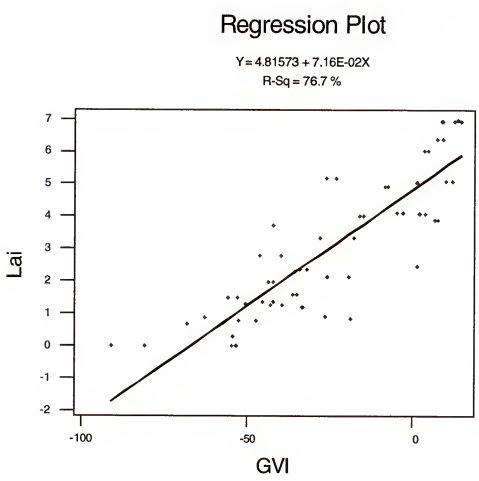

Figure 5-5. Regression plot and equation for GVI and LAI.

Table 5-3. Individual brightness values and in situ LAI for 30 verification points.

Band1	Band2	Band3	Band4	Band5	Band7	Lai
74.56	28.78	32.46	66.76	93.79	35.93	0.94
74.39	28.7	32.2	67.21	91.46	35.09	1.36
72.14	27.71	30.43	62.71	77.29	29.14	2.05
73.44	28.39	29.49	67.34	81.73	29.22	1.88
79.13	30.65	34.56	67.57	92.52	36.79	1.68
74.1	28.98	31.95	62.62	86.16	33.57	1.54
73.42	28.93	32.79	63.38	93.53	34.86	1.36
74.02	29.31	34.35	62.29	106.04	43.06	0.5
63.21	23.61	22.04	46.5	42.56	14.18	1.58
61.08	21.79	20	45.82	39.26	12.48	1.45
64.11	23	22.12	44.05	50.03	17.82	2.77
62.49	22	20.35	42.42	40.48	12.35	2.79
62.89	21.16	20.07	39.91	40.7	14.63	2.72
64.93	23.57	22.91	45.57	46.73	17.02	2.66
61.13	20.4	18.88	39.48	36.47	13.42	2.45
60.08	21.2	17.92	40.28	36.35	12.78	2.35
62.46	22	20.2	40.97	39.25	13	1.65
62.05	21.05	19.02	40.44	36.46	11.32	2.2
62.1	21.63	20	38.26	38.33	14.95	2.16
68.21	25.14	23.07	70.66	63.98	20	4.01
68.2	25.2	22.7	76	59.8	15.79	2.97
65.25	25.57	19.82	79.58	56.02	16.29	3.29
66.36	26	19.98	81.36	57.12	16.35	3.52
66.29	25.01	21.43	74.06	56.61	17.94	5.29
68.12	25.71	21.14	76.24	56.22	17.57	3.51
68.21	25.14	23.07	70.66	63.98	20	4.01
69.03	25.41	23.98	71.61	67.21	22.5	3.27
69.28	26.14	24.29	78.42	71.09	22.95	3.34
70	26.54	24.54	81.46	70	23	3.39
68.12	24.92	20.78	75.57	52.8	17.13	5.38

Table 5-4. Vegetation indices values of 30 verification points.

Lai	NDVI	SAVI	SR	GVI
0.940	0.346	0.344	2.057	-42.529
1.360	0.352	0.350	2.087	-40.178
2.050	0.347	0.345	2.061	-32.117
1.880	0.391	0.389	2.283	-31.621
1.680	0.323	0.322	1.955	-42.529
1.540	0.324	0.323	1.960	-39.605
1.360	0.318	0.316	1.933	-43.861
0.500	0.289	0.288	1.813	-55.238
1.580	0.357	0.354	2.110	-14.285
1.450	0.392	0.389	2.291	-11.372
2.770	0.331	0.329	1.991	-21.730
2.790	0.352	0.349	2.085	-14.663
2.720	0.331	0.328	1.989	-17.302
2.660	0.331	0.329	1.989	-18.822
2.450	0.353	0.350	2.091	-14.141
2.350	0.384	0.381	2.248	-12.961
1.650	0.340	0.337	2.028	-15.142
2.200	0.360	0.357	2.126	-12.932
2.160	0.313	0.311	1.913	-17.047
4.010	0.508	0.505	3.063	-13.441
2.970	0.540	0.537	3.348	-5.789
3.290	0.601	0.598	4.015	-0.291
3.520	0.606	0.603	4.072	0.024
5.290	0.551	0.548	3.456	-5.463
3.510	0.566	0.563	3.606	-3.904
4.010	0.508	0.505	3.063	-13.441
3.270	0.498	0.496	2.986	-15.902
3.340	0.527	0.524	3.228	-13.806
3.390	0.537	0.534	3.319	-11.315
5.380	0.569	0.566	3.637	-2.117

methods (NDVI, SAVI, SR; Figures 5-6, 5-7, 5-8). The RMSE of estimating LAI less than 3.0 was 0.690, 0.693, and 0.657 for NDVI, SAVI and SR respectively. When estimating *in situ* LAI values greater than 3.0, RMSE values increased to 0.998, 0.998, and 0.964 for NDVI, SAVI, and SR respectively. LAI predicted from GVI regression did not appear to have the same type of gap of at LAI values of 3.0 (Figure 5-9). However, GVI was less accurate than other regression methods when estimating LAI values less than 3.0 (RMSE = 1.25), and slightly more accurate when estimating LAI values greater than 3.0 (RMSE = 0.935). LAI values predicted from the linear regression functions are summarized in Table 5-5.

Overall, the regression method with the lowest RMSE was the simple ratio (SR) (RMSE = 0.773; Table 5-6). The second most accurate regression method was NDVI (RMSE = 0.806; Table 5-7), followed by SAVI (RMSE = 0.808; Table 5-8), and the all band regression (RMSE = 0.863; Table 5-9). The worst regression method was GVI as a predictor of LAI (RMSE= 1.155; Table 5-10).

Artificial Neural Network

An artificial neural network (ANN) was created and trained with the *in situ* LAI measurements as the output data and the remote sensor data as the input data. The ANN was created using the spectral reflectances of the six Landsat Thematic Mapper bands. The network was trained with different numbers of hidden layers. After each network training, network error values were output to determine network accuracy. The most accurate network was used to predict LAI in the 30 verification points.

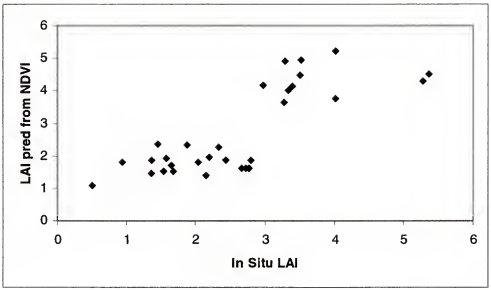

Figure 5-6. Scatter plot of predicted LAI and in situ LAI using NDVI.

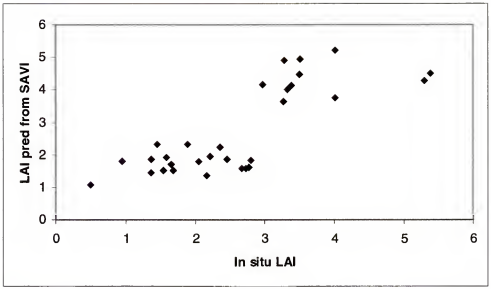

Figure 5-7. Scatter plot of predicted LAI and in situ LAI using SAVI

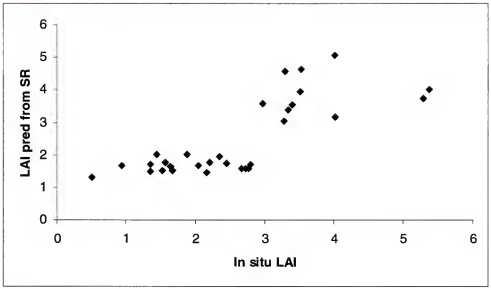

Figure 5-8. Scatter plot of predicted LAI and in situ LAI using SR.

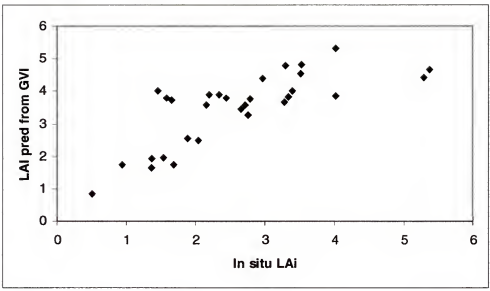

Figure 5-9. Scatter plot of predicted LAI and in situ LAI using GVI.

Table 5-5. Estimated LAI values from each regression function.

Lai	Pr. NDVI	Pr. SAVI	Pr. Sr	Pr. GVI	Pr. 6 band
0.940	1.789	1.789	1.678	1.753	1.772
1.360	1.868	1.868	1.723	1.922	1.970
2.050	1.800	1.798	1.684	2.503	2.316
1.880	2.340	2.338	2.012	2.538	2.485
1.680	1.515	1.516	1.529	1.753	2.699
1.540	1.528	1.527	1.536	1.963	1.794
1.360	1.453	1.452	1.496	1.657	1.260
0.500	1.100	1.099	1.320	0.838	0.126
1.580	1.925	1.915	1.757	3.786	1.839
1.450	2.357	2.344	2.023	3.996	1.796
2.770	1.615	1.605	1.582	3.250	1.239
2.790	1.861	1.848	1.719	3.759	1.665
2.720	1.607	1.594	1.578	3.569	1.533
2.660	1.609	1.600	1.579	3.460	1.798
2.450	1.878	1.862	1.729	3.797	1.499
2.350	2.258	2.241	1.960	3.882	1.106
1.650	1.714	1.701	1.637	3.725	1.552
2.200	1.966	1.951	1.781	3.884	1.758
2.160	1.396	1.382	1.467	3.588	1.238
4.010	3.763	3.760	3.160	3.847	3.354
2.970	4.157	4.154	3.579	4.398	4.318
3.290	4.902	4.900	4.561	4.794	3.883
3.520	4.957	4.955	4.645	4.817	4.142
5.290	4.292	4.289	3.738	4.422	3.740
3.510	4.471	4.468	3.960	4.534	4.203
4.010	3.763	3.760	3.160	3.847	3.354
3.270	3.648	3.645	3.047	3.670	3.330
3.340	3.998	3.997	3.403	3.821	3.652
3.390	4.120	4.120	3.537	4.000	4.126
5.380	4.506	4.502	4.004	4.663	4.529

Table 5-6. Individual RMS errors for SR regression

Lai	LAI Pred. from SR	SR RMS
0.940	1.678	0.545
1.360	1.723	0.132
2.050	1.684	0.134
1.880	2.012	0.018
1.680	1.529	0.023
1.540	1.536	0.000
1.360	1.496	0.019
0.500	1.320	0.673
1.580	1.757	0.031
1.450	2.023	0.329
2.770	1.582	1.410
2.790	1.719	1.146
2.720	1.578	1.304
2.660	1.579	1.169
2.450	1.729	0.520
2.350	1.960	0.152
1.650	1.637	0.000
2.200	1.781	0.176
2.160	1.467	0.480
4.010	5.061	1.104
2.970	3.579	0.371
3.290	4.561	1.616
3.520	4.645	1.266
5.290	3.738	2.408
3.510	3.960	0.202
4.010	3.160	0.723
3.270	3.047	0.050
3.340	3.403	0.004
3.390	3.537	0.022
5.380	4.004	1.893

Table 5-7. Individual NDVI RMS errors for each point.

Lai	LAI Pred from NDVI	RMS NDVI
0.940	1.789	0.721
1.360	1.868	0.258
2.050	1.800	0.063
1.880	2.340	0.211
1.680	1.515	0.027
1.540	1.528	0.000
1.360	1.453	0.009
0.500	1.100	0.359
1.580	1.925	0.119
1.450	2.357	0.822
2.770	1.615	1.334
2.790	1.861	0.863
2.720	1.607	1.238
2.660	1.609	1.105
2.450	1.878	0.327
2.350	2.258	0.008
1.650	1.714	0.004
2.200	1.966	0.055
2.160	1.396	0.584
4.010	5.210	1.440
2.970	4.157	1.408
3.290	4.902	2.599
3.520	4.957	2.064
5.290	4.292	0.995
3.510	4.471	0.924
4.010	3.763	0.061
3.270	3.648	0.143
3.340	3.998	0.433
3.390	4.120	0.532
5.380	4.506	0.765

Table 5-8. Individual RMS errors for SAVI regression.

Lai	LAI Pred. from SAVI	RMS SAVI
0.940	1.789	0.720
1.360	1.868	0.258
2.050	1.798	0.063
1.880	2.338	0.210
1.680	1.516	0.027
1.540	1.527	0.000
1.360	1.452	0.008
0.500	1.099	0.359
1.580	1.915	0.112
1.450	2.344	0.799
2.770	1.605	1.358
2.790	1.848	0.887
2.720	1.594	1.268
2.660	1.600	1.125
2.450	1.862	0.345
2.350	2.241	0.012
1.650	1.701	0.003
2.200	1.951	0.062
2.160	1.382	0.605
4.010	5.211	1.443
2.970	4.154	1.403
3.290	4.900	2.591
3.520	4.955	2.059
5.290	4.289	1.002
3.510	4.468	0.918
4.010	3.760	0.063
3.270	3.645	0.141
3.340	3.997	0.432
3.390	4.120	0.532
5.380	4.502	0.771

Table 5-9. Individual RMS errors for six band regression.

Lai	LAI Pred. from All Band	RMS All Band
0.940	1.772	0.692
1.360	1.970	0.372
2.050	2.316	0.071
1.880	2.485	0.366
1.680	2.699	1.038
1.540	1.794	0.065
1.360	1.260	0.010
0.500	0.126	0.140
1.580	1.839	0.067
1.450	1.796	0.119
2.770	1.239	2.343
2.790	1.665	1.265
2.720	1.533	1.410
2.660	1.798	0.743
2.450	1.499	0.904
2.350	1.106	1.547
1.650	1.552	0.010
2.200	1.758	0.195
2.160	1.238	0.850
4.010	5.717	2.915
2.970	4.318	1.817
3.290	3.883	0.352
3.520	4.142	0.386
5.290	3.740	2.402
3.510	4.203	0.481
4.010	3.354	0.430
3.270	3.330	0.004
3.340	3.652	0.097
3.390	4.126	0.541
5.380	4.529	0.724

Table 5-10. Individual RMS errors for GVI regression

Lai	LAI Pred. from GVI	RMS GVI
0.940	1.753	0.661
1.360	1.922	0.316
2.050	2.503	0.205
1.880	2.538	0.433
1.680	1.753	0.005
1.540	1.963	0.179
1.360	1.657	0.088
0.500	0.838	0.114
1.580	3.786	4.869
1.450	3.996	6.483
2.770	3.250	0.231
2.790	3.759	0.939
2.720	3.569	0.721
2.660	3.460	0.640
2.450	3.797	1.814
2.350	3.882	2.346
1.650	3.725	4.305
2.200	3.884	2.835
2.160	3.588	2.038
4.010	5.312	1.694
2.970	4.398	2.040
3.290	4.794	2.262
3.520	4.817	1.681
5.290	4.422	0.754
3.510	4.534	1.048
4.010	3.847	0.026
3.270	3.670	0.160
3.340	3.821	0.231
3.390	4.000	0.372
5.380	4.663	0.515

The network architecture found to be the most accurate after training with TM bands 1-5 and 7 contained three hidden layers. Based on the RMSE of all the methods, the ANN trained with six band brightness values (Six Band ANN RMSE = 0.672; Table 5-11) was the most accurate technique to measure LAI using remotely sensed imagery.

The scatter plot of actual and predicted LAI values (Figure 5-10) does not reveal the same kind of gap that was evident when the ratio based VIs and six-band regression were used to estimate LAI. When used to estimate LAI values < 3.0, ANN RMSE was 0.552, and 0.863 when estimating LAI values greater than 3.0.

Overall Accuracy

The measurement technique with the smallest RMSE was determined to be the most accurate estimator of LAI using remotely sensed data. Table 5-12 lists *in situ* LAI values and calculated VIs for each method. Results show that ANN techniques are the most accurate method to remotely estimate LAI of all of the methods (Figure 5-11). Regression using SR produced the second most accurate results. This may be due to the simple nature of the near infrared to red ratio. All of the regression methods produced similar results, but NDVI and GVI were the least accurate VI estimators of LAI. Ironically, NDVI was the method of choice for many remote sensing LAI studies.

It was originally thought that six-band regression would be more accurate than VI regression, but using six-bands regression to estimate LAI did not perform well. It is not well understood why six-band regression was so poor, but it may be hypothesized that the different ecosystems represent quite different spectral responses for each band. For example, the middle infrared band is sensitive to water. The xeric sandhills and sand

Table 5-11. Individual NDVI RMS errors for each point.

Lai	Lai pred. from ANN	ANN RMS
0.940	1.214	0.075
1.360	1.361	0.000
2.050	1.911	0.019
1.880	2.152	0.074
1.680	1.934	0.065
1.540	1.449	0.008
1.360	0.983	0.143
0.500	0.503	0.000
1.580	2.516	0.876
1.450	2.372	0.850
2.770	1.851	0.845
2.790	2.392	0.158
2.720	2.223	0.247
2.660	2.387	0.075
2.450	2.197	0.064
2.350	2.054	0.088
1.650	2.359	0.503
2.200	2.577	0.142
2.160	2.088	0.005
4.010	5.320	1.716
2.970	4.340	1.877
3.290	4.209	0.845
3.520	4.494	0.949
5.290	3.925	1.863
3.510	4.565	1.113
4.010	3.389	0.386
3.270	3.222	0.002
3.340	3.394	0.003
3.390	3.877	0.237
5.380	4.808	0.327

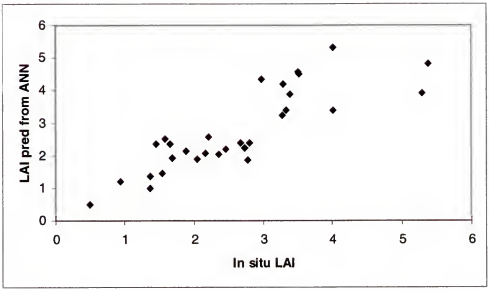

Figure 5-10. Scatter plot of predicted LAI and in situ LAI using ANN.

Table 5-12. Summary of each methods LAI estimate.

Lai	Pr. NDVI	Pr. SAVI	Pr. Sr	Pr. GVI	Pr. 6 band	Pr. ANN
0.940	1.789	1.789	1.678	1.753	1.772	1.214
1.360	1.868	1.868	1.723	1.922	1.970	1.361
2.050	1.800	1.798	1.684	2.503	2.316	1.911
1.880	2.340	2.338	2.012	2.538	2.485	2.152
1.680	1.515	1.516	1.529	1.753	2.699	1.934
1.540	1.528	1.527	1.536	1.963	1.794	1.449
1.360	1.453	1.452	1.496	1.657	1.260	0.9825
0.500	1.100	1.099	1.320	0.838	0.126	0.5032
1.580	1.925	1.915	1.757	3.786	1.839	2.516
1.450	2.357	2.344	2.023	3.996	1.796	2.372
2.770	1.615	1.605	1.582	3.250	1.239	1.851
2.790	1.861	1.848	1.719	3.759	1.665	2.392
2.720	1.607	1.594	1.578	3.569	1.533	2.223
2.660	1.609	1.600	1.579	3.460	1.798	2.387
2.450	1.878	1.862	1.729	3.797	1.499	2.197
2.350	2.258	2.241	1.960	3.882	1.106	2.054
1.650	1.714	1.701	1.637	3.725	1.552	2.359
2.200	1.966	1.951	1.781	3.884	1.758	2.577
2.160	1.396	1.382	1.467	3.588	1.238	2.088
4.010	3.763	3.760	3.160	3.847	3.354	3.389
2.970	4.157	4.154	3.579	4.398	4.318	4.34
3.290	4.902	4.900	4.561	4.794	3.883	4.209
3.520	4.957	4.955	4.645	4.817	4.142	4.494
5.290	4.292	4.289	3.738	4.422	3.740	3.925
3.510	4.471	4.468	3.960	4.534	4.203	4.565
4.010	3.763	3.760	3.160	3.847	3.354	3.389
3.270	3.648	3.645	3.047	3.670	3.330	3.222
3.340	3.998	3.997	3.403	3.821	3.652	3.394
3.390	4.120	4.120	3.537	4.000	4.126	3.877
5.380	4.506	4.502	4.004	4.663	4.529	4.808

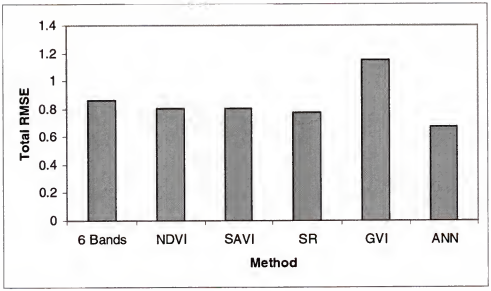

Figure 5-11. RMSE values of each LAI estimation method.

pine scrub, and mesic hammocks may have influenced this band differently. However, the most accurate method, ANN, also used six bands to estimate LAI.

Each estimation method was more accurate when *in situ* LAI was < 3.0, as RMSE values for each increased above this threshold. However, when the ANN was used to estimate LAI, the RMSE remained relatively low, and maintained the lowest RMSE < and >= 3.0.

Discussion

Estimating biophysical characteristics of forested ecosystems over landscape scale areas using remote sensing data is valuable because of the amount of land cover conversion that is currently occurring and the effects of conversion on landscape scale ecology (Curran and Foody, 1994). Knowledge of biophysical characteristics of vegetation at the landscape and regional scales is necessary to describe energy and mass fluxes at the Earth's surface using global circulation models, carbon cycle models, and water models (Weiss and Baret, 1999). The methods used here have shown that a principal biophysical variable, LAI, may be estimated using remote sensor data.

The results suggest that LAI is estimated more accurately when remotely sensed data is used with ANNs. Statistical techniques have been used in many studies to estimate LAI with remote sensor data, but this study has shown that ANNs are more accurate than these methods. Using ANNs to estimate LAI could enhance the accuracy of many published studies that have relied on VI regression to estimate LAI (e.g., (Herwitz et al. 1990; Liu and Huete, 1995; Chen and Cihlar, 1996; Carlson and Riply, 1997; Lymburner et al., 2000). To enhance these studies, ANNs would need to be

created and trained using representative ecosystem *in situ* LAI samples, and then used to estimate LAI in other image areas.

While each method appeared to have a gap at in situ LAI = 3.0, the ANN method exhibited the smallest gap. Almost all of the in situ LAI measurements below 3.0 were measured in pinelands (sandhills or sand pine scrub ecosystems), and those values > 3.0 were measured in hammocks. This may be due to the different kinds of soils, leaf inclination angles, and understory vegetation types that are not taken into account in the models.

The ability to estimate LAI over large areas is useful for monitoring human-induced and natural changes in forest ecosystems. Such estimates can be used to examine how the changes affect landscape and regional scale ecology. To this end, two studies were carried out that use these methods to analyze forest ecology over landscape scale areas. These two studies are described in the next chapter.

CHAPTER 6
ECOLOGICAL STUDIES

Human-induced land cover changes are occurring at increasing rates. This conversion often affects biophysical characteristics of ecosystems such as leaf area index (LAI). This chapter details two ecological studies mentioned in Chapter 1 that examine landscape scale LAI. The titles of the two studies are:

1. Leaf Area Index, Fire, and Succession in Longleaf Pine/Turkey Oak Sandhills.
2. Comparisons of the Urban Forests of Gainesville and Ocala, Forida.

In addition to answering important ecological questions, these two studies demonstrate the utility of the models presented in the technical development of the LAI estimators. The first study was chosen because of my interest in the ecology of longleaf pine/turkey oak sandhills. Specifically, I am interested in the fire ecology of these ecosystems, and how fire affects their spatial distribution. Fire is often not well understood as a tool to manage ecosystems. Studies that allow people to recognize the importance of fire to maintain native ecosystems are important to allow people to understand the role of fire and support its use as a management tool.

The second study was chosen because urban forests provide many aesthetic, environmental, and monetary benefits. These benefits include oxygen production, reduced wind velocity and noise levels, reduced erosion, shade, and filtration of dust and

particulate matter in the air. Local government polices can influence the amount of urban forests in communities. This study analyzes the LAI of two urban forest found in cities with different tree ordinances.

LEAF AREA INDEX, FIRE, AND SUCCESSION IN LONGLEAF PINE/TURKEY OAK SANDHILLS

Introduction

Longleaf pine/turkey oak sandhills are adapted to low-intensity fires at intervals of one - ten years. Fire allows these systems to out-compete invasive species from nearby ecosystems. Without fire, sandhills will usually succeed into southern mixed hardwood forests (Myers, 1990). As a result of succession, the biophysical properties of sandhills such as leaf are index (LAI) may increase to become more like the climax southern mixed hardwood forest system. Therefore, it may be possible to predict succession in the sandhills by examining the spatial distribution of LAI as recorded in remotely sensed imagery.

By mapping sandhill LAI, managers can find areas that are in danger of being transformed into xeric/mesic hammocks because of lack of fire, and these areas could be targeted for prescribed burns if maintenance of sandhill ecosystems is an objective.

The Importance of Fire

Fire is important because it affects characteristics such as plant species distribution, nutrient availability, vertebrate and invertebrate populations, and soil structure (Whelan, 1995). Fire is a naturally occurring phenomenon that has maintained ecological communities such as longleaf pine (*Pinus palustris*) savannas in the

southeastern coastal plain and the plant and animal species that live there (Aber and Melillo, 1991; Platt, 1998).

Human responses to fire usually reflect the confusion between positive and negative effects. Aboriginal peoples throughout the world frequently used fire to reduce pests, prepare the land for farming, or increase forage for grazing animals. Fire remains a major land-clearing practice in the tropics. Until recently, fire suppression has been an accepted forest management practice throughout most of the Western world (Aber and Melillo, 1990).

Early naturalists noted that longleaf pine savannas with accompanying turkey oak (*Quercus laevis*) and wiregrass (*Aristida beyrichiana*) represented the most extensive forest type on the southeastern coastal plain from Texas to North Carolina including peninsular Florida (Frost, Walker, and Peet, 1986; Platt, 1998). These naturalists described the landscape as open, with low herbaceous ground cover and visibility for more than one kilometer through longleaf pine that often did not form a full canopy (Platt, 1998). Longleaf pine/turkey oak sandhills (LLP/TO) habitat began to change in character and disappear from the landscape following European settlement mostly because they were used for both open pasture and converted to agriculture (Platt, 1998). In fact, deforestation rates of the region were higher than that currently observed in the tropics (Simberloff, 1993). Presently, only 3% of the former LLP/TO area exists because of factors such as fire suppression, overcutting, habitat fragmentation, favoring other pine species, and other human activities (Platt, 1998; Carter et al., 1999). Due to this intense reduction, sandhill ecosystems are considered to be critically endangered (Noss, LaRow, and Scott, 1995).

Beginning in the 1960s, controlled burns were more often used as a management tool in the longleaf pine and turkey oak sandhill ecosystems. Fire began to be used more frequently as a management tool because perceptions of fire began to change as people realized that native ecosystems were being lost as a result of fire suppression.

Sandhills have erroneously been characterized as a fire subclimax because of probable succession to hammocks succession in the absence of fire. However, succession following the clearing of upland pine or mixed hardwood forests does not pass through a longleaf pine/turkey oak (LLP/TO) stage after abandonment. Rather, many severely cut-over pine stands and agricultural fields that once supported longleaf pine have failed to return to the original vegetation cover even after frequent burning (Platt, 1998; Myers, 1990). Therefore, instead of being a subclimax community, LLP/TO is an intricately evolved ecosystem closely linked to fire (Myers, 1990; Platt, 1998).

Longleaf pine is pyric, or fire-controlled, allowing longleaf pine to thrive only in areas that regularly burn. For example, following germination and seedling establishment, longleaf pine saplings remain in grass stage for 3 to 20 years (Figure 2-2). During the grass stage, a large taproot is produced that contains great quantities of stored photosynthates. The apical bud is embedded in the surrounding needles that are resistant to burning. After reaching a critical size, the seedling begins very rapid height growth, up to one meter per year. This growth results from the frequent surface fires that the plant has adapted to, and allows the plant to quickly grow above the levels of most ground fires (Aber and Melillo, 1991; Myers, 1990).

Frequent, low-intensity fires help longleaf pine/turkey oak communities compete with tree species from adjacent communities because they remove the understory of

invasive hardwoods and other pines, while only sometimes scorching and seldom killing the longleaf pines. Without fire, these communities are invaded by species from adjacent xeric and mesic upland communities (Myers, 1990). This results in declining fire-adapted species and the overall vegetation changing to either a mesic or xeric hardwood forest (Figure 6-1; Myers, 1990; Platt, 1998). Therefore, I hypothesized that in the absence of fire, leaf area index (LAI) in Longleaf Pine/Turkey Oak (LLP/TO) communities will increase (as will primary productivity) because LLP/TO are not able to compete without the aid of fire. In addition, fire suppression will result in higher soil cation exchange capacity (CEC) and amounts of available calcium (Platt, 1998). Given these characteristics, sandhill health may be correlated with low LAI values.

Although sandhills typically have lower tree species diversity than hammocks, they contain more overall plant species diversity than hammocks because of an extremely species-rich herbaceous layer. In fact, sandhills are among the most species-rich communities outside of the tropics (Carter et al., 1999).

Sandhills typically burn every 1 to 10 years, and longleaf pine has become adapted to frequent fires with characteristics such as thick bark, a fire resistant juvenile 'grass' stage, and masting after fires (Platt, 1998). Turkey oak also has thick bark that helps protect from ground fires. Wiregrass (*Aristida beyrichiana*) is associated with LLP/TO communities in Florida and depends on fires in the growing season to stimulate regeneration and to reduce competition (Myers, 1990). The frequency, regularity, season, and intensity of burn can have differing effects on the species, structure, and species abundance of LLP/TO sandhills. For example, the abundance and stature of deciduous oaks in sandhills may be proportional to the mean length of fire-return interval: the longer

2 Years

7 Years

17 Years

Figure 6-1. Sandhill succession from date of last burn.

the interval, the more prevalent the oaks. Furthermore, when fire is excluded, species from surrounding ecosystems invade, fire-adapted species decline, and the vegetation gradually changes to either a xeric or mesic hardwood (Myers, 1990).

Many vertebrate species are dependent on LLP/TO communities. These include the endangered red-cockaded woodpecker (*Picoides borealis*) and the Florida mouse (*Podomys floridanus*) (Platt, 1998). Other animals in danger are gopher tortoise (*Gopherus polyphemus*), indigo snake (*Drymarchon corais*), and Sherman's fox squirrel (*Sciurus niger shermanii*) (Carter et al., 1999; Myers, 1990; Platt, 1998). These animals serve important ecological functions such as seed dispersal and nest cavity construction. The gopher tortoise is considered a keystone species because its burrows provide refuge to many other species of vertebrates and invertebrates that, in turn, serve other important roles in the sandhills.

This study examines the hypothesis that sandhills that have not recently burned will have higher LAI values than those that have recently burned. Specifically, sandhills that have not had prescribed or natural burns over a period > 10 years should exhibit higher LAI values than those that have had fires within the last ten years. This hypothesis is tested using artificial neural networks (ANNs) and remotely sensed imagery.

Methods

Study Area

Katharine Ordway Preserve and the contiguous Carl Swisher Sanctuary consist of approximately 3,642 ha located in western Putnam County, Florida, 42 km east of

Gainesville, Florida. The Preserve contains several different native ecosystems including extensive LLP/TO sandhills and hammocks. Prescribed burns have been used as a management tool for the preservation of native ecosystems in the preserve.

Sandhill soils range from droughty, coarse sands to calcareous, phosphatic sand clays that occur on level to sloping terrain. Most soils lack any profile development and are classed as sandy entisols (quartzipsamments) derived from marine aeolian or fluvial sand deposits (Myers, 1990). The soils are generally excessively drained, highly permeable, and low in nutrients. The variation in texture, drainage, fertility, and development of soils is further evidence of the primary importance of fire (Myers, 1990).

The climate in north central Florida is characterized by a long growing season with mild winters. Average January and July temperatures are 12.5° C and 27° C, respectively. Precipitation averages 130 cm per year, with the majority falling as rain between May and September.

Burn History

The University of Florida has recorded the burn history in the Katharine Ordway Preserve (J. Eisenberg, personal communication, 1999; Figure 6-2). This history was digitized into a vector geographic information system (GIS) layer and was correlated with leaf area index (LAI) that was calculated using a remote sensing derived Artificial Neural Network (ANN) technique developed in Chapter 5.

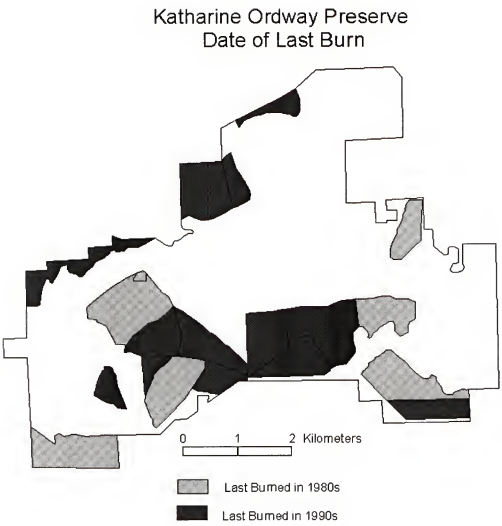

Figure 6-2. Burn map of Katharine Ordway Preserve.

Satellite Imagery

Landsat Thematic Mapper data was used for this study (WRS Path 17 Row 39; 22 March 1997). Landsat 5 TM was launched on 1 March 1984 and was built, as the name implies, for the identification and classification of landscape land uses and patterns (Aber and Melillo, 1991; Jensen, 2000). Whereas previous remote sensing systems recorded electromagnetic energy in bands determined to be most useful for general vegetation and geology studies (e.g., Landsat Multispectral Scanner), Landsat TM bands were selected after years of analysis for their value in measuring water penetration, discrimination of vegetation type and vigor, plant and soil moisture measurement, and other applications. The TM bands were selected to make use of the dominant factors controlling leaf reflectance, such as leaf pigmentation, leaf and canopy structure, and moisture content as described above in Chapter 3 (Figure 3-1). Landsat TM remote sensing bands have been used to measure vegetation characteristics (Teillet, Staenz, and Williams, 1997; Huete et al., 1997). Various transformations of the data from TM bands have been shown to accurately measure forest LAI (Gholz, Vogel, Cropper Jr., McKelvey, Ewel, Tesky, and Curran, 1991; Curran, 1994; Fassnacht et al., 1997).

Artificial Neural Network and LAI Measurements

The use of artificial neural networks (ANN) for remote sensing data interpretation has been motivated by the realization that the human brain is very efficient at processing information (Keiner and Yan, 1998). Remotely sensed data sets processed by ANN based classifiers have included images from the Landsat Multispectral Scanner (MSS; Benediktsson et al., 1990), Landsat Thematic Mapper (TM; Yoshida and Omatu, 1994),

and other sensors. In nearly all cases, the ANN classifiers have proven superior to conventional classifiers, often recording accuracy improvements in the range of 10-20% (Gopal et al., 1999; for a discussion on ANNs, see Chapter 3).

The ANN used for this study was created and trained using 64 *in situ* LAI values as the network output. These 64 LAI measurements were made using an AccuPar Ceptometer that measures photosynthetically active radiation above and below forest canopies, and calculates LAI based on the Beer-Lambert Extinction law that states that as PAR passes through a canopy, its intensity decreases exponentially with increasing amount of cover (Larcher, 1975). LAI *in situ* measurements were made at each corner of a 20 x 20 m quadrat in each cardinal direction and averaged. GPS points were taken in the middle of each quadrat to extract brightness values from Landsat TM imagery. Brightness values obtained from TM bands 1-5, and 7 were used as input to the ANN and used to predict LAI.

Data Analysis

Sandhill sites that were recently burned (<= 10 years), and sandhill sites that have not recently burned (> 10 years) were selected to use in the analysis by generating one hundred random points for each of the two time periods. Remote sensing brightness values were extracted from six Thematic Mapper bands using a GIS interpolation point program developed in the ArcView Avenue scripting language (Appendix B). These brightness values were run through the ANN, and LAI values were estimated for each point. Estimated LAI values were then placed into a difference of means t-test (Agresti and Finlay, 1997).

Results

Results indicate that LAI is greater in longleaf pine /turkey oak (LLP/TO) sandhill communities that have not burned in more than 10 years. Communities that burned in the last ten years have lower estimated LAI values (mean = 0.90; s.d. = 0.40) than those that last burned more than ten years ago (mean = 1.54; s.d. = 0.92). LAI values predicted from the ANN clearly demonstrated this relationship ($n = 100$, $t = 7.61$; $p < 0.00001$). The higher standard deviation of sandhills that have not burned in the last 10 years may be related to the proximity of southern mixed hardwood forests or hammocks. Sandhills that are adjacent to hammocks will succeed more quickly into hardwood forests and will have higher LAI values than sandhills that are not adjacent to hammocks.

A surface LAI image was created using the ANN (Figure 6-3; Appendix C). This LAI map demonstrates several characteristics. Those sandhills that burned within ten years of sampling had lower LAI values than those that did not burn within the last ten years. As noted above, hammocks surround many of the sandhills used in this study. These hammocks had higher LAI values than sandhills.

Discussion

This study tested whether LAI of longleaf pine/turkey oak sandhills increases as a result of time since last burn. The study was based on the use of satellite remote sensing data, an artificial neural network, and a *t*-test. Sandhills are native ecosystems in the southeastern coastal plain that maintain a variety of plants and animals, and they currently occupy only 3% of their previous extent (Platt, 1998). Sandhills depend on

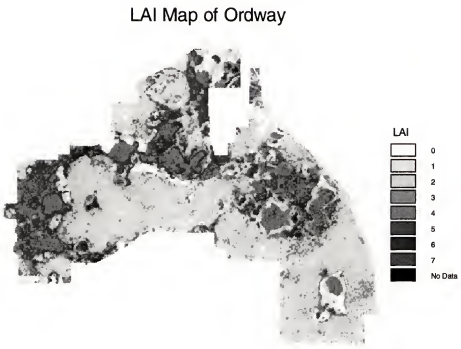

Figure 6-3. LAI map of Katharine Ordway Preserve calculated using an artifical neural network and six bands of Landsat Theamtic Mapper brightness values.

regular fires to out compete invasive species from adjacent communities. When fire is suppressed, sandhills will generally succeed to southern mixed hardwood forests containing many different species of hardwoods and other pines. As a result, the biophysical characteristics of the ecosystem will also change. For example, LAI increases in the absence of fire. Furthermore, if fire in sandhills are suppressed, fuel loads increase, thus increasing the possibility of severe crown fires like Florida experienced in the summer of 1998.

The results from this study suggest that sandhill succession may be able to be mapped using remotely derived LAI estimates. Foresters may inexpensively generate LAI maps using the same techniques used in this study. These maps could be presented to landowners as evidence that their land may be in danger of succession or catastrophic burning if a prescribed burn is not carried out. The mapping of areas of sandhill succession could be a useful tool that forest managers and conservationists can use to determine those areas where prescribed burns are needed to stave off succession in the southeastern coastal plain. This could aid an ecosystem that now occupies a fraction of its former area.

Conclusions

In summary, the following conclusions may be reached:

1. The LAI of sandhills is positively correlated with date of last burn.
2. Sandhills that have not burned in the last ten years have lower LAI values than sandhills that have burned in the last ten years.
3. Sandhill LAI is able to be mapped using satellite remote sensing data and artificial neural networks.
4. Sandhill succession can be predicted using LAI values.

A COMPARISON OF THE URBAN FORESTS IN GAINESVILLE AND OCALA, FL

Introduction

There has been a worldwide trend of migration of rural people into urban areas (Kato Okohari, and Brown, 1997). For example, urban population has increased from 40% of the United States' total population in 1900 to 75% in 1990 (U.S. Census, 1990). Florida has seen an even greater proportional increase in urban population. In 1900, Florida's population was 20.3% urban, which increased to 84.8% of the total state population in 1990 (U.S. Census, 1990). Given this urban influx, concern about environmental quality and the long-term livability of urban areas is now an important issue for planners because urban conditions are often stressful and unhealthy for humans (Flores, Pickett, Zipperer, Pouyat, and Pirani, 1998). Within this paradigm, the incorporation of ecological knowledge is necessary to protect and restore a wide variety of environmental resources including, urban forests. Studies have confirmed that 'tree cities' help residents cope with stress, provide a pleasant backdrop, and filter urban air (Ridd and Liu, 1998; Flores et al., 1998).

This study compares the leaf area index (LAI) of two cities that are geographically close and similar in many ways (e.g., climate, culture, industry), yet have different amounts of forest canopy. LAI, m^2 of leaves per m^2 of ground, is an important forest biophysical variable that indicates canopy cover and is correlated with canopy-atmosphere gas exchange.

Urban forestry is defined by Blouin and Comeau (1993) as:

> the sustained planning, planting, protection, maintenance, and care of trees, forests, green space, and related resources in and around cities and communities for economic, environmental, social, and public health benefits for people. The definition includes retaining trees and forest cover as urban populations expand into surrounding rural areas and restoring critical parts of the urban environment after construction. Expansion at the urban/rural interface raises environmental and public health safety concerns, as well as opportunities to create educational and environmental links between urban people and nature. In addition, urban and community forestry includes the development of citizen involvement and support for investments in long-term on-going tree planting, protection, and care programs.

Urban forests are valued for both aesthetic and ecological reasons. Most of the aesthetic values are non-monetary benefits such as pleasant landscape, peace and quiet, screening and privacy, and recreation opportunities (Tyrvainen and Vaananen, 1998; Kennard, Putz, and Niederhofer, 1996). For example, trees can make urban settings more attractive (Sheets and Manzer, 1991) and have a positive impact on residents' moods (Hull, 1992). Trees have been found to increase property values (Anderson and Cordell, 1985), and inner-city residents have said that trees favorably influence their decisions about where to live (Getz, Karow, and Kielbaso, 1982). These studies suggest that natural features like trees may improve urban environments (Summit and Sommer, 1998. More municipal governments now realize that trees make their communities more livable. Because of this, urban tree management has progressed from simply appreciating trees to actively managing both the number and types of trees.

Urban forests also have several environmental benefits. Trees absorb gaseous pollutants through leaf stomata and can dissolve or bind water-soluble pollutants onto moist leaf surfaces. Tree canopies intercept particulates and reduce local air temperatures

in the summer and increase temperatures in the winter (McPherson, Scott, and Simpson, 1998). Urban trees may reduce air ozone concentrations, either by direct or indirect absorption of ozone or other pollutants such as NO2, or by reducing air temperature, which reduces hydrocarbon emission and ozone formation rates (McPherson et al., 1998).

Urban areas are warmer than the relatively cooler surrounding non-urban countryside. This phenomenon, known as the urban heat island, is caused by deforestation and the replacement of the land surface by nonevaporative and nonporous materials such as concrete and asphalt. In addition, air conditioning systems can introduce a significant amount of heat into the urban landscape. The result of air conditioning is reduced evapotranspiration and an increase in urban temperature (Jensen, 2000). Two studies (Quattrochi and Ridd, 1999; Lo, Quattrochi, and Luvall, 1997) evaluated several cities using thermal remote sensing data to document the heat island effect. They found that during the daytime hours commercial land cover exhibited the highest temperatures followed by services, transportation, and industrial areas. Conversely, the lowest daytime temperatures were found over water, vegetation, and agricultural land use. At night, commercial, services, industrial, and transportation land cover types cooled relatively rapidly, but their predawn early morning temperatures were still slightly higher than those of vegetated and agricultural areas. Sailor (1995) found that the urban heat island was diminished when vegetation was increased in a climate model of the Los Angeles area. Quattrochi and Luvall (1999) found that the few urban forests located throughout Atlanta, Georgia had a significant dampening effect on the urban heat island. This is particularly evident in northeast Atlanta where the residential tree canopy is extensive. This information has been used to: 1) model the relationship

between Atlanta urban growth, land cover change, and the development of the heat island through time; 2) model the relationship between Atlanta urban growth, land cover change, and air quality through time; and, 3) model the overall effects of urban development on the energy budget across Atlanta (Jensen, 2000). These data can then be used to recommend tree-planting programs.

Sacramento Shade in Sacramento, California, a partnership between the Sacramento Municipal Utility District (SMUD) and the not-for-profit Sacramento Tree foundation annually plants 50,000 trees in residents' yards to reduce air conditioning demand (McPherson et al., 1998). It has turned out to be one of SMUD's most cost-effective energy reducing programs. Deciduous trees provide shade in the summer and let in warming winter sun when their leaves are gone. In fact, a single properly watered tree can have an estimated cooling effect of more than one million BTUs, thus exceeding the output rating of many room air conditioners (McPherson et al., 1998).

Given the importance of urban forests, this study tests whether the urban forest in Gainesville, FL is greater or less than that of Ocala, FL. It is based on digital image processing techniques applied to remotely sensed imagery and the use of an Artificial Neural Network to estimate leaf area index (LAI). The possibility exists that two cities with different LAI would differ in terms of energy use. With the recent increase in prices of fossil-fuel based energy, the urban life of a treed city would be "better" because less money would have to be spent on heating.

Methods

Study Area

Many cities throughout the nation either already have or are beginning to develop and enforce tree ordinances that govern the removal and planting of trees. Two such towns are Gainesville and Ocala are located in north central Florida on the southeastern coastal plain. The climate in north central Florida is characterized by a long growing season with mild winters. Average January and July temperatures are 12.5° C and 27° C respectively.

Gainesville, FL (population 93,969) has adopted a tree ordinance that requires landowners and developers to plant native trees on an area basis (e.g., one tree / 2850 sq. feet). Gainesville's Land Development code contains property design principles that encourage tree preservation, and strict regulations inhibit tree destruction. For example, if trees are planted along roads the Land Development Code separates different types of tree species into large, medium, and small categories, each with it own purpose. Large trees require 15 linear meters spacing and include live *oak (Quercus hemisphearica)*, southern magnolia (*Magnolia grandiflora*), sweetgum (*Liquidambar styraciflua*), and winged elm (*Ulmus alata*). Medium trees are used for streets with a right of way < 25 meters that require 11 linear meters spacing and include blackgum (*Nyssa sylvatica*), bald cypress (*Taxodium distichum*), spruce pine (*Pinus glabra*), and red maple (*Acer rubrum*). Small trees are generally used under power lines and consist of crape myrtle (*Lagerstromia indica*), holly (*Ilex* spp.), hop hornbeam (*Ostrya virginiana*), and ash magnolia (*Magnolia ashei*).

According to the city's general plan, if trees have been displaced due to lot development or construction, it is mandated that one "shade tree" for each 2,850 square feet of gross lot to five acres and one shade tree for each 3,000 square feet of gross lot area over five acres be planted. In addition, Gainesville has implemented species control programs that promote removal of invasive exotic trees such as tallow tree (*Sapium sebiferum*) throughout the city (Putz, Holdnak, and Niederhofer, 1999).

Because of these strict ordinances, Gainesville has been awarded the distinction of "Tree City USA" by the National Arbor Day Foundation for the last 13 years (Putz et al, 1999). This award recognizes the creative and varied programs that help to keep Gainesville well forested.

Ocala, FL is located 40 km south of Gainesville. While Ocala has a tree ordinance that prohibits tree destruction, the ordinance is not as strict as Gainesville's. For example, homeowners with lots < 3 acres that are zoned residential do not need to apply for a tree removal permit. In addition, if a tree is removed it must be replaced, but the ordinance mandates replacement with only a very small tree. Ocala has a smaller population than Gainesville (60,000), but its urban forest is not as extensive. This may be due to the rapid growth that has transformed Ocala from a quiet central Florida town to one that must concern itself with such issues as downtown decay and intensive use of environmental assets. The main differences between the tree ordinances in the two cities are found in Table 6-1.

The two cities are comparable insofar as they are geographically close, have similar climates, have similar total populations, and exhibit similar economies, but Ocala has a pro-growth approach to planning and Gainesville does not. The University of

Table 6-1. Differentiation of tree policies in Gainesville and Ocala, Florida adapted from each cities General Plan.

	Gainesville	**Ocala**
Population	94,000	60,000
Residential tree removal	Trees < 20″ DBH require no permit; 20 – 30″ cedars, loblolly bays, longleaf pines, Florida maples, and red maples require tree removal permits; *all trees* > 30″ require permits	No permit required if lot size < 3 acres and owner does not own adjacent lots.
Land zoned as commercial tree removal	Hardwoods, longleaf pine, and spruce pine > 8″ DBH, and slash pine and loblolly pine > 12″ require permits to remove; *all trees* > 30″ require permits	All regulated trees > 4″ require a permit to be removed.
Agricultural land tree removal	Buffer areas must be maintained on tree plantations	No permit required if land is being used for agriculture
Nuisance tree removal	Free to remove without permit	Free to remove without permit
Cost of tree removal permit	$0	$75
Penalties for illegal tree removal	If trees are removed without a permit, they must be replaced on an inch per inch basis. All healthy trees > 30″ that are not causing structural damage must be replaced on an inch per inch basis	Illegally removed trees can be replaced by multiple trees of at least 3″ where the aggregate DBH of the replacement trees must equal that of the removed trees.
New development	1 shade tree for every 2,850 sq. feet.	Depends on number of trees in area before development. Maximum amount is 1 tree per 3,000 square feet.
How is the ordinance governed?	Full-time arborist and staff	Committee of nine – including three political appointees
When was the Ordinance first implemented?	1982	1989

Florida is located in Gainesville, and both cities are located along Florida's central ridge in the southeastern coastal plain. Given these similarities, these cities are ideal to compare urban forest LAI and its consequences.

Remote Sensor Data

A Geographic Information System (GIS) generated forty random points within the city limits of both Gainesville and Ocala. These points were used to extract Landsat Thematic Mapper (TM) (WRS 17-39 and 17-40, 22 March 1997) interpolated brightness values from bands 1-5, and 7 using a GIS program written in the ArcView Avenue scripting language (Appendix B). Landsat 5 TM was launched on 1 March 1984 and was built, as the name implies, for the identification and classification of landscape land uses and patterns (Aber and Melillo, 1991; Jensen, 2000). Whereas previous remote sensing systems measured in bands determined to be most useful for general vegetation and geology studies (e.g., Landsat Multispectral Scanner), Landsat TM bands were selected after years of analysis for their value in measuring water penetration, discrimination of vegetation type and vigor, plant and soil moisture measurement, and other applications. The TM bands were selected to make use of the dominant factors controlling leaf reflectance, such as leaf pigmentation, leaf and canopy structure, and moisture content (Jensen, 2000; Figure 3-1). Landsat TM data have been used to measure vegetation characteristics (Teillet et al., 1997; Huete et al., 1997). Transformations of data from TM bands have been shown to accurately measure forest LAI (R. Jensen, 2000; Curran, 1994; Gholz et al., 1991; Fassnacht et al., 1997).

LAI Measurements

TM brightness values were transformed using a trained Artificial Neural Network (ANN) that calculates leaf area index (LAI). The ANN was made by Jensen (2000) and trained using *in situ* LAI measurements and Landsat TM brightness values for each of the six bands. To measure *in situ* LAI, photosynthetically active radiation (PAR) was measured using a Decagon Accupar Ceptometer above and below natural forest canopies of 64 sites in north central Florida.

PAR measurements were made on each corner of 20 x 20 m quadrats in each cardinal direction and averaged. GPS points were taken in the middle of the quadrat for later input into the GIS program to extract TM brightness values.

Data Analysis

The Landsat TM brightness values were evaluated in the trained ANN to estimate LAI for each point. The use of artificial neural networks (ANN) for remote sensing data interpretation has been motivated by the realization that the human brain is very efficient at processing information (Atkinson and Tatnall, 1997). Remotely sensed data sets processed by ANN based classifiers have included images from the Landsat Multispectral Scanner (MSS; Benediktsson et al., 1990), Landsat Thematic Mapper (TM; Yoshida and Omatu, 1994), and other sensors. In nearly all cases the ANN classifiers have proven superior to conventional classifiers, often recording accuracy improvements in the range of 10-20% (Gopal et al., 1999; for a discussion on ANNs, see Chapter 3). Each cities' forty points were then placed into a difference of means *t*-test.

Results

Surface LAI maps were generated using the ANN for both Gainesville and Ocala (Figures 6-4 and 6-5; Appendix C). Several trends seem apparent in these maps. Aside from the airport in the northeast, Gainesville appears to have uniform LAI values. Ocala's LAI values appear to vary greatly, and has corridors of high LAI values.

Estimated LAI of Gainesville's urban forest (mean = 4.61; s.d. = 1.27) of the 40 random points was greater than Ocala's urban forest LAI (mean = 2.13; s.d. = 1.20). LAI for the two cities estimated using the Landsat TM data and the Artificial Neural Network were statistically significantly different ($t = 10.17$; $p < 0.00001$). This difference suggests that Gainesville's more stringent policies (Table 6-1) are effective for maintaining tree cover.

The Gainesville tree ordinance has not only contributed to making Gainesville more attractive from a pedestrian perspective, but the ordinance helps to alleviate some of the urban heat island effects and pollution problems. For example, residences in Gainesville use an average of 935-kilowatt hours per month (R. Bauldree, Gainesville Regional Utility, personal communication, 2000). Conversely, Ocala residences use an average of 1,075 kwH per month (J. Henning Ocala Electric Utility, personal communication, 2000). Using the average rate of $0.07524 / kwH, this results in a yearly savings of $126.40 per household. Although other factors could be influencing this such as geographical location, it seems clear that the urban forest contributes to this savings.

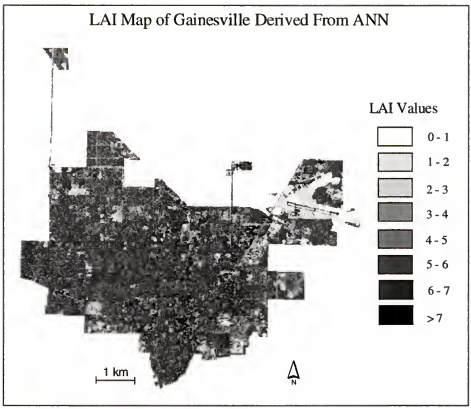

Figure 6-4. LAI surface map of Gainesville derived from ANN.

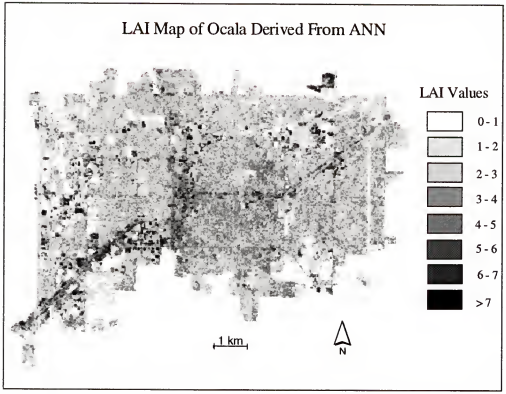

Figure 6-5. LAI surface map of Ocala derived from ANN.

Discussion

The purpose of this study was to estimate the LAI of two central Florida cities' urban forests and explain what effect these forests may be having on energy consumption. The benefits of urban forests are well documented, and using remotely derived imagery and Artificial Neural Networks to estimate LAI, it may be concluded that Gainesville has much higher LAI values in its urban forest than does Ocala. This canopy cover not only benefits Gainesville aesthetically, but it also improves air quality, decreases pollution, and may reduce energy consumption.

Other cities, such as Jacksonville, FL, have recently passed laws that require home builders to either replant or pay for some of the larger trees (> 60 cm diameter breast height) they cut down during subdivision construction. These laws could help alleviate some of the problems of urban areas and increase the quality of life.

Urban planners with LAI maps and data on energy usage by household could determine where the most good would be done by creating incentives for planting larger trees, and where smaller trees might be better. This would allow for allocation of scarce resources (e.g., city funds) in an optimal manner, and it could be rapidly and inexpensively implemented using this approach to LAI mapping.

Future research could focus on the opportunity cost of urban forests and their benefits to society. Perhaps there are some locations where it is not cost-effective to maintain urban forests. These areas may prove to be the exception to the rule, and should be studied. In addition, not all areas are suitable for urban forests, and care must be taken in urban forestry programs to be sensitive to existing cultural customs. Ethnic

backgrounds of individual neighborhoods and the affects of urban forests could also be studied. There may be a correlation between amount of urban forest cover and ethnicity of the neighborhood. Furthermore, different types of trees may be more efficient in air filtration or other benefits. Therefore, different types of trees in urban forests could also be investigated.

Conclusions

The following conclusions can be made:

1. Urban forests with high LAI values and more canopy cover can reduce energy consumption
2. Gainesville's urban forest has higher estimated LAI values than Ocala's urban forest.
3. Municipal policies on tree removal and planting play a factor in the amount of forest cover.
4. Satellite remote sensor data used in conjunction with a well-trained ANN can predict LAI for use in urban forest studies.
5. Urban planners may be able to promote tree planting and preservation by quantifying the amount of energy used in different parts of the city and comparing these amounts with average LAI of the same area.
6. The approach could be applied to urban forests throughout the world provided an ANN is trained using representative ecosystems common to the urban area.

CHAPTER 7
DISCUSSION AND CONCLUSIONS

Discussion

Increased awareness and knowledge of the implications of land cover conversion suggests that environmental modeling will continue to be important to assess impacts of environmental change. Specifically, quantitative information on the distribution of biophysical variables is required for environmental research. For example, in climate modeling, the canopy structure of forests determines fluxes of radiation, water vapor, and sensible heat to the atmosphere (DeFries and Townshend, 1994). Change in forest canopy structure is an important variable in the study of fluxes of greenhouse gases from terrestrial biota to the atmosphere (DeFries and Townshend, 1994), and information on the distribution of canopy characteristics is necessary to accurately measure these changes.

The linking of remotely sensed data with ecosystem biophysical variables is an important contribution to understanding how the earth functions at landscape to regional scales (Curran, 1994). This study has shown that models created to remotely estimate leaf area index (LAI) using *in situ* LAI measurements, ANNs, and remotely sensed data are better than traditional statistical methods. Of the vegetation indices (VIs) studied, the SR vegetation index was the most accurate of the regression predictors. The artificial neural network trained using six TM bands had the lowest root mean square error of all the methods used and was therefore the most accurate method for predicting LAI from

remotely sensed images. This was due to the ANNs' ability to use nonalgorithmic strategies and not rely on linear relationships or normally distributed data.

Most remote sensing studies that have estimated LAI using remote sensing data have used one of the VI regression functions to estimate LAI. In particular, NDVI has been used extensively to estimate LAI (e.g., Fassnacht et al., 1998). This study has shown that each of these regression methods is less accurate than using ANNs to estimate LAI.

These methods can be used to answer important geographical questions by describing LAI dynamics at landscape to regional scales. This use was demonstrated in the two ecological studies of LAI and sandhill succession, and urban forest LAI. These methods could aid land managers, conservationists, foresters, and others in making educated decisions using remotely sensed and therefore inexpensive biophysical data.

In addition, historical LAI maps could be generated using relevant remote sensor data that were taken the same time of year as the scene that was used to train the ANNs. Historic remote sensing data should be radiometrically normalized using techniques described by Heo and FitzHugh (2000). This would allow landscape LAI dynamics to be studied over time.

Using these techniques to estimate LAI, ecological studies may be carried out at the landscape scale. For example, LAI of longleaf pine/turkey oak sandhills can be estimated using ANNs and used as an indicator of sandhill succession. Sandhills are native to the southeastern United States coastal plain, and currently occupy only 3% of their previous extent. Without regular fires, sandhills will succeed into hardwood forests. The longer sandhills go without burning, the higher their LAI values become. Therefore,

LAI measurements can be used to indicate sandhills that are in danger of becoming hardwood forests. For example, LAI surface maps could be generated to aid managers in identifying sandhills that need prescribed burns.

Urban forests are important in part because of their ability to filter air, reduce energy consumption, and increase property values. Municipal policies can affect the amount of forest cover in urban areas. The LAI of the urban forests of two cities in north central Florida were estimated and compared using ANNs. The urban forest in the city with more stringent tree removal policies and stricter replanting rules had much higher LAI values. These higher LAI values helped reduce energy consumption. The method could be used in conjunction with other data to target areas within cities for canopy restoration. Other ecological studies could be done that use ANNs to estimate LAI over local, landscape, regional, and global scales.

Other Sensors

Although Landsat Thematic Mapper (TM) and has good spectral (seven bands) and adequate spatial (30 x 30 m) resolution, other sensors exist that have even better resolution. It is assumed here that the same techniques could be applied to these other sensors. For example, the Advanced Very High Resolution Radiometer (AVHRR) could be used for continental sized studies of LAI. AVHRR has some advantages over TM. For example, while TM has a revisit time of 16 days, AVHRR images the earth twice each day. This allows for great temporal coverage and increases the chances of cloud-free images. AVHRR has a larger instantaneous field of view (1.1 x 1.1 km) that makes it feasible to collect, store, and process continental data sets. AVHRR measures in five

portions of the electromagnetic spectrum (EMS) (red, 0.58 - 0.68 μm; near-infrared, 0.725 - 1.10 μm; middle-infrared 3.55 - 3.93 μm; middle-infrared, 10.30 - 11.30 μm; and thermal infrared, 11.50 - 12.50 μm). This spectral resolution allows for fine radiometric differences to be detected. Conversely, Le Systeme Pour l' Observation de la Terre (SPOT) provides data with much smaller IFOVs (20 x 20 m). Although SPOT only measures in three bands in the spectrum (green, 0.50 - 0.59 μm; red, 0.61 - 0.68 μm; and near-infrared, 0.79 - 0.89 μm) it has been used in vegetation studies. IKONOS provides multispectral data with an IFOV of 4 x 4m. This sensor could allow for much more detailed estimation of canopy parameters as well as for delineating forest type. Hyperspectral sensors such as AVIRIS and MODIS could be implemented in LAI studies. MODIS could provide even more accurate measurement of LAI using the techniques described in this research. MODIS would provide much greater spectral resolution that could take advantage of subtle radiometric changes that TM was unable to identify. Because ANNs can process large sets of data, these sensors could be easily used as input to train ANNs and may provide very accurate estimates of landscape scale LAI.

As long as the sampling methods are modified to match each sensor's resolution, these sensors could map landscape scale LAI. If other sensors are used, special care should be taken so that the *in situ* measurements mirror the IFOV of the sensor being used. For example, AVHRR data has an IFOV of 1.1 x 1.1 km, and *in situ* LAI measurements need to mimic this resolution. In the case of SPOT, *in situ* measurements need to mimic the 20 x 20 m IFOV resolution. Sensors with very high spatial resolution such as IKONOS need to have sampling schemes that are detectable with 4 x 4 m pixels.

As new technologies, techniques, and remote sensors become available, the ability to map and monitor biophysical variables such as LAI will continue to improve. This study has provided a model by which data from other sensors could be applied using appropriate sampling methods.

Conclusions

This dissertation has demonstrated that:

1. Artificial neural networks (ANNs) can be used to estimate landscape scale LAI. Because of their ability to outperform conventional statistical methods.
2. The most accurate regression estimator of LAI was the simple ratio vegetation index.
3. Six band regression did not perform as well as expected in predicting LAI.
4. ANNs are more accurate estimators of LAI than regression functions determined from vegetation indices and all bands.
5. LAI of sandhills is positively correlated with time from last burn, over a ten-year scale.
6. Sandhill LAI can be mapped using satellite remote sensing data and artificial neural networks.
7. Sandhill succession is indicated by increasing LAI values.
8. Urban forests with high LAI values contain more canopy cover.
9. Gainesville's urban forest has higher estimated LAI values than Ocala's urban forest, and this translates into higher energy costs for Ocala residents.
10. Municipal policies on tree conservation, removal, and replanting play a factor in the LAI of urban forests.
11. Cities with higher average LAI use less energy to mitigate urban heat-island effects.
12. ANNs and remote sensing provide a means to estimate landscape scale LAI

Future Research

Future research could focus on integrating landscape scale LAI measurements into GIS ecosystem process models. Such process models include Hybrid v. 3.0 that estimates the daily cycling of carbon, nitrogen, and water within the biosphere and between the biosphere and atmosphere, the Regional Ecosystem Simulation System (RESSys) that models regional ecosystem dynamics, and the FOREST-BGC model that estimates the amount net carbon gained or lost in forested ecosystems. These models depend on accurate LAI estimates, and the techniques developed in this research could provide more accurate LAI estimate than are currently being used.

ANNs are able to incorporate almost any type of data in any format, so other variables could be included in the estimation of LAI. These variables might include soil type, precipitation, temperature, and adjacent land cover.

Landscape ecology studies could be implemented using the techniques described. For example, sandhill LAI may also be positively correlated with sandhill patch size, shape, and number. Boundaries and edges of these patches may affect patch LAI as well (Forman, 1995). By first analyzing the characteristics of sandhill patches, more accurate LAI measurements may be made.

Specific studies that could be improved by the techniques developed in this research include studies that estimate LAI based on regression functions (e.g., Fassnacht et al., 1997; Herwitz et al., 1990; Carlson and Ripley, 1997). By implementing ANNs into these studies, their results could be enhanced, and more accurate conclusions could be made.

APPENDIX A
CALCULATION OF LOCAL GVI COEFFICIENTS

According to Jackson (1983) local coefficients can be calculated for the "Tasseled Cap" transformation using the following procedure. To obtain the first index (brightness index), a line through soil data points must be derived. A minimum of two soil point values (preferably with very different brightness values, e.g. wet and dry soil) must be recorded for all six bands. The differences between the dry (X_{sd}) and the wet (X_{sd}) soil points are

$$b_i = (X_{sd} - X_{sw})_i$$

for each of the n bands. The vector ($b_1 \ldots, b_n$) is then normalized to form a unit vector by dividing each of its components by the normalization factor B, where

$$B = (\sum_{i=1}^{n} b_i^2)^{1/2}$$

Then,

$$A_{1,i} = b_i / B$$

are the brightness coefficients.

The second index (greenness index) begins by choosing a green vegetation data point in all bands and forming the differences between these points and any point along the soil line. Then ,

$$g_i = (X_g - X_s)_i - D_{2,1} A_{1,i}$$

where

$$D_{2,1} = \sum_{i=1}^{n} (X_g - X_s)_i A_{1,i}$$

This ensures that the vector $(g_i \ldots, g_n)$ is orthogonal to the soil line vector $(b_i \ldots, b_n)$. The normalization factor is

$$G = (\sum_{i=1}^{n} g_i^2)^{1/2}$$

The greenness coefficients are

$$A_{2,i} = g_i / G$$

And greenness can then be calculated by

$$GN = A_{2,1} X_1 + A_{2,2} X_2 + \ldots + A_{2,n} X_n$$

For this study the following values were extracted from the image:

	Band 1	Band 2	Band 3	Band 4	Band 5	Band 7
Dry Soil	79	29	32	59	93	36
Wet Soil	101	48	69	65	168	110
Green Veg	69	26	20	97	59	14

These values yielded the following equation to calculate greenness:

Greenness = (-0.169841374617434 * Band 1) +

(-0.0460316513600325 * Band 2) +

(-0.19960319253551 * Band 3) +

(0.680953690308967 * Band 4) +

(-0.577381306585965 *Band 5) +

(-0.36349203365472 * Band 7)

APPENDIX B
GIS INTERPOLATED POINT EXTRACTION

The GIS program written to obtain interpolated point brightness values from each of the spectral bands follows.

```
' get view doc
v = av.getactivedoc
if (v.is(view).not) then
  msgbox.error("The active document must be a view.","")
  return nil
end

' find point theme
'thmlst={}
'for each t in v.getthemes
'  if (t.is(ftheme) and (t.getftab.getshapeclass.getclassname="Point")) then
'    tc = t.clone
'    thmlst.add(tc)
'  else
'    continue
'  end
'end
```

```
'pthm = msgbox.list(thmlst,"Select the point theme.","Point theme")
'if (pthm=nil) then msgbox.error("You must select a point theme.","") return nil end
'pthmName = pthm.getname
'pftab = pthm.getftab

' get active point theme
pthm = v.getactivethemes.get(0)
if ((pthm.is(ftheme).not) or (pthm.getFtab.getshapeclass.getclassname="Point").not) then
  msgbox.error("You must have a point theme as the active theme.","")
  return nil
end
pftab = pthm.getftab
pthmName = pftab.getName

newfile = MsgBox.Input("Enter New Field Name:","Field Name","Grid1")


' check to see if point ftab is already being edited
if (pftab.IsBeingEditedWithRecovery) then
  msgbox.error(pthmName++"is currently being edited.  You should finish"+nl+"editing
and then run this script again.","")
  pftab =nil
  pthm = nil
```

```
  pthmName = nil
  return nil
end

' use selected features if present
pSel = pftab.getSelection.clone
if (pSel.count > 0) then
  theData = pSel
  else
  theData = pftab
end

' get surface theme
sthmlst={}
for each s in v.getthemes
  if ((s.is(gtheme)) or (s.is(stheme))) then
    sc = s.clone
    sthmlst.add(sc)
  end
end

sthm = msgbox.list(sthmlst,"Select the surface theme.","Surface theme")
if (sthm = nil) then msgbox.error("You must select a surface to continue.","")
```

```
return nil end


if (sthm.is(stheme)) then
  surf = true
  s = sthm.getsurface
  else
  surf = false
  g = sthm.getgrid
end
' make the x,y and z fields if they do not already exist
fldlst={}
if (pftab.findfield("xval") = nil) then
  xfld = field.make("xval",#FIELD_DOUBLE, 19, 6)
  fldlst.add(xfld.clone)
end
if (pftab.findfield("yval") = nil) then
  yfld = field.make("yval",#FIELD_DOUBLE, 19, 6)
fldlst.add(yfld.clone)
end
'if (pftab.findfield("zval") = nil) then
  zfld = field.make(newfile,#FIELD_DOUBLE, 15, 2)
fldlst.add(zfld.clone)
'end
```

```
' define shape field
shpfld = pftab.findfield("shape")

' start editing the feature table
pftab.setEditable(true)
'   add appropriate fields
    pftab.addfields(fldlst)
  for each p in theData
'   get point and then values
    pc = pftab.returnvalue(shpfld,p).clone
    if (surf) then
      zvalue = s.elevation(pc.returnProjected(v.getprojection))
      else
      zvalue = g.pointvalue(pc,v.getprojection)
    end
    xval = pc.returnprojected(v.getprojection).getx
    yval = pc.returnprojected(v.getprojection).gety
'   set values
    pftab.setvalue(pftab.findfield("xval"),p,xval)
    pftab.setvalue(pftab.findfield("yval"),p,yval)
    pftab.setvalue(pftab.findfield(newfile),p,zvalue)
  end
```

```
pFTab.SetEditable(false)

pftab.flush

pftab.refresh

rpt= table.make(pftab)

rpt.getwin.activate


' clean up and show the results

fldlst.empty

g = nil
```

APPENDIX C
ANN IMAGE CREATION

Artificial Neural Networks are still relatively new in the remote sensing community and are somewhat difficult to integrate with current image processing software. The image data and ANNs used in this project were no exception. Therefore, to create LAI surface images using ANNs required several steps.

1. Convert each TM band from 8-bit binary data to ASCII text.
2. Open the newly converted text image as a text file in Microsoft Word.
3. Copy each of the digital numbers and paste them in a Minitab Worksheet with 5,000,000 cells.
4. Export the worksheet as a tab-delimited text file.
5. Import the data set into Statsitica Neural Networks to run through the already created NN.
6. Export the estimated LAI values to a Minitab Worksheet.
7. Export the worksheet as a tab-delimited text file.
8. Import the tab-delimited text file into Erdas Imagine.

There were probably other ways to complete this task, but this method proved the most efficient for this project. As ANNs become more common in the remote sensing literature, it is hoped that image processing software will be easier to integrate with ANNs.

REFERENCES

Aber, J.D. and J.M. Melillo. 1991. *Terrestrial Ecosystems*. Saunders College Publishing, Chicago.

Abrahamson, W.G. and D.C Hartnett. 1990. "Pine flatwoods and dry prairies." In *Ecosystems of Florida*. R.L. Myers and J.J. Ewel. Orlando, University of Central Florida Press, pp.103-149.

Agresti, A. and B. Finlay. 1997. *Statistical Methods for the Social Sciences*. Prentice Hall: Upper Saddle River, NJ.

Ahern, F.J., T. Erdle, D.A. Maclean, and I.D. Kneppeck. 1991. "A quantitative relationship between forest growth rates and thematic mapper reflectance measurements." *International Journal of Remote Sensing*, 12:387-400.

Anderson, L. and H. Cordell. 1985. "Residential property values improve by landscaping with trees." *Scandinavian Journal of Applied Forestry* 9:162-166.

Asrar, G., M. Fuchs, E.T. Kanemasu, and J.L. Hatfield. 1984. "Estimating absorbed phtosynthetic radiation and leaf area index from spectral reflectance in wheat." *Agronomy Journal*, 76:300-306.

Badhwar, G.D., R.B. MacDonald, F.G. Hall, and J.G. Carnes. 1986. "Spectral characterization of biophysical characteristics in a boreal forest: relationship between Thematic Mapper band reflectance and leaf area index for aspen." *IEEE Transactions on Geoscience and Remote Sensing*, GE-24:322-326.

Benediktsson, J.A., P.H. Swain, and O.K. Ersoy. 1990. "Neural network approaches versus statistical methods in classification of multisource remote sensing data." *IEEE Transactions on Geoscience and Remote Sensing*, 28:540-551.

Birthe, G.S. and G. McVey. 1968. "Measuring the color of growing turf with a reflectance spectrophotometer." *Agronomy Journal*, 60:640-643.

Bischof, H., W. Shneider, and A.J. Pinz. 1992. "Multispectral classification of Landsat-images using neural networks." *IEEE Transactions on Geoscience and Remote Sensing*, 30:482-490.

Blouin G. and R. Comeau. 1993. First Canadian Urban Forests Conference. Canadian Forestry Association, p.4.

Bonan, G.B. 1993. "Importance of leaf area index and forest type when estimating photosynthesis in boreal forests." *Remote Sensing of Environment*, 43:303-314.

Box, E.O., B.N. Holben, and V. Kalb. 1989. "Accuracy of the AVHRR vegetation index as a predictor of biomass, primary produductivity and net CO2 flux." *Vegatatio*, 80:71-89.

Brockway, D.G. and K.W. Outcalt. 1998. "Gap-phase regeneration in longleaf pine wiregrass ecosystems." *Forest Ecology and Mangement* 106:125-139.

Campbell, G.S. and J.M. Norman. "The description and measurement of plant canopy structure." In *Plant canopies: their growth, form and function.* G. Russel, B. Marshall, and P.G. Garvis, Eds. New York, Cambridge University Press.

Campbell, J.B. 1996. *Introduction to Remote Sensing*. New York: Guilford.

Carlson, T.N. and D.A. Ripley. 1997. "On the relation between NDVI, fractional vegetation cover, and leaf area index." *Remote Sensing of Environment*, 62:241-252.

Carter, R.E., M.D. MacKenzie, and D.H. Gjerstad. 1999. "Ecological land classification in the southern loam hills of south Alabama." *Forest Ecology and Mangement* 114:395-404.

Chason, J.W., D.D. Baldocchi, and M.A. Huston. 1991. "A comparison of direct and indirect methods for estimating forest canopy leaf area." *Agriculture Forestry and Meteorology* 57:107-128.

Chen, J.M. and J. Cihlar. 1996. "Retrieving leaf area index of boreal conifer forests using landsat TM images." *Remote Sensing of Environment*, 55:153-162.

Chen, J.M. 1996. "Optically-based methods for measuring seasonal variation of leaf area index in boreal conifer stands." Agriculture and forest

Choudhury, B.J. 1987. "Relationships between vegetation indices, radiation absorption, and net photosynthesis evaluated by a sensitivity analysis." *Remote Sensing of Environment*, 22:209-233.

Cihlar, J., L. St-Laurent, and J.A. Dyer. 1991. "Relation between the normalized difference vegetation index and ecological variables." *Remote Sensing of Environment*, 35:279-298.

Clevers, J.G.P.W. 1988. "The derivation of a simplified reflectance model for the estimation of leaf area index." *Remote Sensing of Environment*, 25:53-69.

Clevers, J.G.P.W. 1989. "The application of a weighted infrared-red vegetation index for estimating leaf area index by correcting for soil moisture." *Remote Sensing of Environment*, 29:25-37.

Clough, B.F., J.E. Ong, and G.W. Gong. 1997. "Estimating leaf area index and photosynthetic production in mangrove forest canopies." Oecologia.

Crist, E.P. 1985. "A Thematic Mapper tasseled cap equivalent for reflectance factor data." *Remote Sensing of Environment*, 17:301-306.

Curran, P.J. 1994. "Attemps to drive ecosystem simulation models at local to regional sclaes." In *Environmental Remote Sensing from Regional to Global Scales*, G.M. Foody and P.J. Curran eds. New York, Wiley.

Curran, P.J., J.L. Dungan, and H.L. Gholz. 1992. "Seasonal LAI in slash pine estimated with Landsat TM." *Remote Sensing of Environment*, 39:3-13.

Curran, P.J. and G. M. Foody. 1994. "Environmental issues at regional to global scales." In *Environmental Remote Sensing from Regional to Global Scales*, G.M. Foody and P.J. Curran eds. New York, Wiley

Datt, B. 1998. "Remote sensing of chlorophyll a, cholorphyll b, chlorophyll a+b, and total carotenoid content in Eucalyptus leaves." *Remote Sensing of Environment*, 66:111-121.

Decagon. *Accupar PAR Ceptometer - Operator's Manual*. Ver. 2.1.

DeFries, R.S. and J.R.G. Townshend. 1994. "Global land cover: comparison of ground-based data sets to classifications with AVHRR data." In *Environmental Remote Sensing From Regional to Global Scales*. G. Food and P. Curran, eds, New York, Wiley, pp. 84-110.

DeGloria, S., A. Benson, K. Dummer, and E. Fakhoury. 1985. "Evaluation of Thematic Mapper data for mapping forest, agriculture, and soil resources." *Advances in Space Research*, 5:31-39.

De Wilde, P. 1996. *Neural Network Models: An Analysis*. London: Springer.

Ellsworth, D.S. and P.B. Reich. 1993. "Caonpy structure and vertical patterns of photosynthesis and related leaf traits in a deciduous forest." Oceologia 96:169-178.

Elvridge, C.D. and R.J.P. Lyon. 1985. "Influence of rock-soil spectral radiation on assessment of green biomass." *Remote Sensing of Environment*, 17:265-279.

Ewel, K.C. 1990. "Swamps." In *Ecosystems of Florida*. R.L. Myers and J.J. Ewel. Orlando, University of Central Florida Press, pp.281-323.

Ezra, C.E., L.R. Tinney, and R.D. Jackson. 1984. "Considerations for implementing vegetation indices in agricultural applications." *Proceedings*, American Society of Photogrammetry, 526-536.

Fassnacht, K.S., S.T. Gower, M.D. MacKenzie, E.V. Nordheim, and T.M. Lillesand. 1997. "Estimating the leaf area index of North Central Wisconsin forests using the Landsat Thematic Mapper." *Remote Sensing of Environment*, 61:229-245.

Flores, A., S.T.A. Pickett, W.C. Zipperer, R.V. Pouyat, and R. Pirani. 1998. "Adopting a modern ecological view of the metropolitan landscape: the case of a greenspace system for the New York City region." *Landscape and Urban Planning*, 39:295-308.

Friedl, M.A. and C.E. Brodley. 1997. "Decision tree classification of land cover from remotely sensed data." *Remote Sensing of Environment*, 61:399-409.

Frost, C.C., J. Walker, and R. K. Peet. 1986. "Fire-dependent savannas and prairies of the southeast: original extent, preservation status and management problems." In *Wilderness and Natural Areas in the Eastern United States: A Management challenge*. D.L. Kulhavy and R.H. Conner, eds. Nacogdoches, Texas, Center for Applied Studies, Stephen F. Austin State University.

Getz, D., A. Karow, and J.J. Kielbaso. 1982. "Inner city preferences for trees and urban forestry program." *Journal of Arboriculture* 8:258-263.

Gholz, H.L. 1982. "Environmental limits on aboveground net primary production, leaf area, and biomass in vegetation zones of the Pacific Northwest." *Ecology*, 63:469-481.

Gholz, H.L, S.A. Vogel, W.P. Cropper Jr., K. McKelvey, K.C. Ewel, R.O. Tesky, and P.J. Curran. 1991. "Dynamics of canopy structure and light interception in *Pinus ellioti* stands, North Florida." *Ecological Monographs*, 61:33-51.

Gholz, H.L., P.J. Curran, J.A. Kupiec, and G.M. Smith. 1997. "Assessing leaf area and canopy biochemistry of Florida pine plantations using remote sensing." In *The Use of Remote Sensing in the Modelling of Forest Productivity.* G.H. Gholz. K. Nakane, and H. Shimoda eds. Boston: Kluwer. pp. 3-22.

Gong, P., P. Ruiliang, and B. Yu. 1997. "Conifer species recognition: an exploratory analysis of *in situ* hyperspectral data." *Remote Sensing of Environment*, 62:189-200.

Gopal, S., and C. Woodcock. 1996. "Remote sensing of forest change using artificial neural networks." *IEEE Transactions on Geoscience and Remote Sensing* 34:398-404.

Gopal, S., C.E. Woodcock, and A.H. Strahler. 1999. "Fuzzy neural network classification of global land cover from a 10 AVHRR data set." *Remote Sensing of Environment*, 67:230-243.

Gower, S.T. and J.M. Norman. 1991. "Rapid estimation of leaf area index in conifer and broad-leaf plantations." *Ecology*, 72:1896-1900.

Green, E.P., P.J. Mumby, A.J. Edwards, C.D. Clark, and A.C. Ellis. 1997. "Estimating leaf area index of mangroves from satellite data." *Aquatic Botany* 58:11-19.

Haykin, S. 1994. *Neural Networks a Comprehensive Foundation*. Prentice-Hall, Upper Saddle River, NJ.

Hepner, G.F., T. Logan, N. Ritter, and N. Bryant. 1989. "Artificial neural network classification using a minimal training set: comparison to conventional supervised classification." *Photogrammetric Engineering and Remote Sensing* 56:469-473.

Herwitz, S.R., D.L. Peterson, and J.R. Eastman. 1990. "Thematic mapper detection of changes in the leaf area of closed canopy pine plantations in central Massachusetts." *Remote Sensing of Environment*, 29:129-140.

Heo, J. and T.W. FitzHugh. 2000. "A standardized radiometric normalization method for change detection using remotely sensed imagery." *Photogrammetric Engineering and Remote Sensing* 66:173-181.

Holben, B.N., C.J. Tucker, and C.J. Fan. 1980. "Spectral assessment of soybean leaf area and leaf biomass." *Photogrammetric Engineering and Remote Sensing*, 46:651-656.

Huete, A.R., E.F. Post, and R.D. Jackson. 1984. "Soil spectral effects on 4-space vegetation discrimination." *Remote Sensing of Environment*, 15:155-165.

Huete, A.R., G. Hua, J. Qi, A. Chehbouni, W.J.D. Van Leeuwen. 1992. "Normalization of multidirectional red and NIR reflectances with the SAVI." *Remote Sensing of Environment*, 41:143-154.

Huete, A.R. and H.Q. Liu. 1994. "An error and sensitivity analysis of the atmospheric and soil-correcting variants of the NDVI for the MODIS-EOS." *IEEE Transactions on Geoscience and Remote Sensing*, 32:897-904.

Huete, A.R., H.Q. Liu, K. Batchil, and W. van Leeuwen. 1997. "A comparison of vegetation indices over a global set of TM images for EOS-MODIS." *Remote Sensing of Environment*, 59:440-451.

Hull, R.B. 1992. "Brief encounters with urban forests produce moods that matter." *Journal of Aboriculture* 18:322-324.

IGBP, 1990. *The International Geosphere-Biosphere Program: A study of global change: the initial core projects*. International Geosphere-Biosphere Programme, Stockholm.

Jackson, R.D. 1983 "Spectral indices in n-Space." *Remote Sensing of Environment*, 13:409-421.

Jensen, J.R. 1983. "Biophysical remote sensing." *Annals, Association of American Geographers*, 73:111-132.

Jensen, J.R. 1996. *Introductory Digital Image Processing: A Remote Sensing Perspective*. Prentice-Hall, Englewood Cliffs, NJ.

Jensen, J.R. 2000. *Remote Sensing of the Environment: An Earth Resources Perspective*. New Jersey, Prentice-Hall.

Jensen, J.R. and F. Qui. 2000. "Predictive modeling of coniferous forest age using statistical and artificial neural network approaches applied to remote sensor data." *International Journal of Remote Sensing*, Forthcoming.

Jin, Y.Q. and C. Liu. 1997. "Biomass retrieval from high-dimensional active/passive remote sensing data using artificial neural networks." *International Journal of Remote Sensing*, 18:971-979.

Justice, C.O., J.R. Townshend, B.N. Holder, and C.J. Tucker. 1985. "Analysis of the phenology of global vegetation using meteorological satellite data." *International Journal of Remote Sensing*, 6:1271-1318.

Kato, Y. M. okohari, and R.D. Brown. 1997. "Integration and visualization of the ecological value of rural landscapes in maintaining the physical environment of Japan." *Landscape and Urban Planning* 39:69-82.

Kauth, R.J. and G.S. Thomas. 1976. "The tasseled cap – a graphic description of the spectral-temporal development of agricultural crops as seen be Landsat." *Proceedings*, Machine Processing of Remotely Sensed Data, West Lafayette, IN: Laboratory for the Applications of Remote Sensing, 41-51.

Keiner L.E. and X. Yan. 1998. "A neural network model for estimating sea surface chlorophyll and sediments from thematic mapper imagery." *Remote Sensing of Environment*, 66:153-165.

Kennard, D.K., F.E. Putz, and M. Niederhofer. 1996. "The precictability of tree decay based on visual assessments." *Journal of Arboriculture*, 22:249-254.

Larcher, W. 1975. *Physiological Plant Ecology*. New York: Springer-Verlag.

Lawrence, R.L. and W.J. Ripple. 1997. "Comparisons among vegetation indices and bandwise regression in a highly disturbed, heterogeneous landscape: Mount St. Helens, Washington." *Remote Sensing of Environment*,64:91-102.

Lillesand, T.M. and R.W. Keifer. 2000. *Remote Sensing and Image Interpretation*. New York: Wiley and Sons.

Li. X, and A.H. Strahler. 1985. "Geometric-optical modeling of a confer forest canopy." *IEEE Transactions on Geoscience and Remote Sensing*,GE-23:705-721.

Li, X and A.H. Strahler. 1992. "Geometric-optical bidirectional reflectance modeling of the discrete crown vegetation canopy: effect of crown shape and mutual shadowing." *IEEE Transactions on Geoscience and Remote Sensing*, 30:276-292.

Liu, Q. and A. Huete. 1995. "A feedback based modification of the NDVI to minimize canopy background and atmospheric noise." *IEEE Transactions on Geoscience and Remote Sensing*, 33:457-465.

Lo, C.P., D.A Quattrochi, and J.C. Luvall. 1997. "Application of high resolution thermal infrared remote sensing data and GIS to asses the urban heat island effect." *International Journal of Remote Sensing* 18:287-304.

Lymburner, L, P.J. Beggs and C.R. Jacobson. 2000. "Estimation of canopy-average surface-specific leaf area using Landsat TM data." *Photogrammetric Engineering and Remote Sensing* 66:183-191.

Manly, B.F. 1992. *The Design and Analysis of Research Studies*. Cambridge, Cambridge University Press.

Mather, P.M. 1987. *Computer processing of remotely sensed images: an introduction*. New York, Wiley and Sons.

McPherson, E.G., K.I. Scott, and J.R. Simpson. 1998. "Estimating cost effectiveness of residential yard trees for improving air quality in Sacramento, California, using existing models." *Atmospheric Environment* 32:75-84.

Miller, R.L. and J.S. Kahn. 1962. *Statistical Analyses in the Geological Sciences*. New York, John Wiley and Sons.

Murdiyarso, D. and U.R. Wasrin. 1995. "Estimating land use change and carbon relase from tropical forests conversion using remote sensing technique." *Journal of Biogeography*, 22:715-721.

Myers, R. L. 1990. "Scrub and High Pine." In *Ecosystems of Florida*. R.L. Myers and J.J. Ewel. Orlando, University of Central Florida Press, pp.150-193.

Nel, E.M. and C.A. Wessman. 1993. "Caonopy transmittance models for estimating forest leaf area index." *Canadian Journal of Forest Resources* 23:2579-2586.

Nelson, R. N. Horning, and T.A. Stone. 1987. "Determining the rate of forest conversion in Mato Grosso, Brazil, using Landsat MSS and AVHRR data." *International Journal of Remote Sensing*, 8:1767-1784.

Nezry, E., e. Mougin, A. Lopes, and J.P. Gastellu-Etchegorry. 1993. "Tropical vegetation mapping with combined visible and SAR spaceborne data." *International Journal of Remote Sensing*, 14:2165-2184.

Noss, R.F., E.T. LaRow, and J.M. Scott. 1995. "Endangered ecosystems of the United States: a preliminary assessment of loss and degradation." Biological Report 28, National Biological Survey, 58 pp.

Pearson, R.L. and L.D. Miller. 1972. "Remote mapping of standing crop biomass for estimation of the productivity of the shortgrass prairie." In *Proceedings of the Eighth International Symposium on Remote Sensing of Environment*, Environmental Research Institute of Michigan, Ann Arbor, MI, pp. 1357-1381.

Pierce, L.L. and S.W. Running. 1988. "Rapid estimation of coniferous forest leaf area index using a portable integrating radiometer." *Ecology*, 69:1762-1767.

Pinty, B., C. Leprieur, and M.M. Verstraete.1993. "Towards a quantitative interpretation vegetation indices - Part 1: Biophysical canopy properties and classical indices." *Remote Sensing Review* 7:127-150.

Platt, W.J. 1998. "Southeastern pine savannas." In *Savannas, Barrens, and Rock Outcrop Plant Communities of North America*, Cambridge University Press, New York.

Platt, W.J. and M.W. Schwartz. 1990. "Temperate hardwood forests." In Ecosystems of Florida. R.L. Myers and J.J. Ewel. Orlando, University of Central Florida Press, pp194-229.

Putz, F.E., M. Holdnak, and M. Niederhofer. 1999. "Controlling invasive exotics: a tallow tree replacement program campaign in Florida." *Journal of Arboriculture* 25:98-101.

Quattrochi, D.A. and M.K. Ridd. 1994. "Measurement and analysis of thermal energy responses from discrete urban surfaces using remote sensing data." *International Journal of Remote Sensing* 15:1991-2022.

Quattrochi, D.A. and M. K. Ridd. 1998. "Analysis of vegetation within a semi-arid environment using high spatial resolution airborne thermal infrared remote sensing data." *Atmospheric Environment* 31:19-33.

Quattorchi, D.A. and J.C. Luvall. 1999. "High spatial resolution airborne multispectral thermal infrared data to support analysis and modeling tasks in the EOS IDS Project Atlanta." http://wwwghcc.msfc.nasa.gov/atlanta/.

Ridd, M.K. and J. Liu. 1998. "A comparison of four algorithms for change detection in an urban environment." *Remote Sensing of Environment* 63:95-100.

Ripple, W.J. 1994. "Determining coniferous forest area and forest fragmentation with NOAA-9 Advanced Very High Resolution Radiometer data." *Photogrammetric Engineering and Remote Sensing*, 60:533-540.

Rouse, J.W., R.H. Haas, J.A. Schell, and D.W. Deering. 1974. "Monitoring vegetation systems in the Great Plains with ERTS." *Proceedings*, Third Earth Resources Technology Satellite-1 Symposium, Greenbelt: NASA SP-351, 3010-3017.

Roy, P.S., B.K. Ranganath, P.G. Diwakar, T.P.S. Vohra, S.K. Bhan, I.J. Singh, and V.C. Pandian. 1991. "Tropical forest type mapping and monitoring using remote sensing." *International Journal of Remote Sensing*, 12:2205-2225.

Ruimy, A., B. Saugier, G. Dedieu. 1994. "Methodology for the estimation of terrestrial net primary production from remotely sensed data." *Journal of Geophysical Research*, 99:5263-5283.

Rummelhart, D.E., G.E. Hinton, and R.J. Williams. 1986. "Learning representations by back-propagating algorithms." *Nature*, 323:533-536.

Running, S.W., D.L. Peterson, M.A. Spanner, and K.B. Teuber. 1986. "Remote sensing of coniferous forest leaf area." *Ecology*, 67:273-276.

Running, S.W., R.R. Nemani, D.L. Peterson, L.E. Band, D.F. Potts, L.L. Pierce, and M.A. Spanner. 1989. "Mapping regional forest evapotranspiration and photosynthesis by coupling satellite data with ecosystem simulation." *Ecology*, 70:1090-1101.

Running, S.W., C.O. Justice, V. Solomonson, D. Hall, J. Barker, Y.J. Kaufmann, A.H. Strahler, A.R. Huete, J.P. Muller, V. Vanderbilt, Z.M. Man, P. Teillet, and D. Carneggie. 1994. "Terrestrial remote sensing science and algorithms planned for EOS/MODIS." *International Journal of Remote Sensing* 15:3587-3620.

Sailor, D.J. 1995. "Simulated urban climate response to modifications in surface albedo and vegetative cover." *Journal of Applied Meteorology* 34:1694-1704.

Sellers, P.J., C.J. Tucker, G.J. Collatz. 1994. "A global 10x10 NDVI dataset for climate studies. Part 2- the adjustment of the NDVI and generation f global fields of terrestrial biophysical parameters." *International Journal of Remote Sensing*, 15:3519-3545.

Sellers, P., S. Los, and C. Tucker. 1995, "A revised land surface parameterization (SiB2) for atmospheric GCMs, part 2: the generation of global fields of terrestrial biophysical parameters from satellite." Journal of Climatology 9:706-737.

Sheets, V. and C. Manzer. 1991. "Affect, cognition, and urban vegetation: some affects of adding trees along city streets." *Environment and Behavior* 23:285-304.

Simberloff, D. 1993. "Species-area and fragmentation effects on old-growth forests: prospects for longleaf pine communites. *Proceedings Tall Timbers Fire Ecology Conference*, 18:1-13.

Smith, F.W., D.A. Sampson, and J.N. Long. 1991. "Comparison of leaf area index estimates from tree allometrics and measured light interception." *Forest Science*, 37: 1682-1688.

Spanner, M.A., L.L. Pierce, D.L. Peterson, and S.W. Running. 1990. "Remote sensing of temperate coniferous forest leaf area index: the influence of canopy closure, under story vegetation and background reflectance." *International Journal of Remote Sensing*, 11:95-111.

Summit, J. and R. Sommer. 1998. "Urban tree-planting programs - a model for encouraging environmentally protective behavior." *Atmospheric Environment* 32:1-5.

Teillet, P.M., K. Staenz, J.J. Williams. 1997. "Effects of spectral, spatial, and radiometric characteristic on remote sensing vegetation indices of forested regions." *Remote Sensing of Environment*, 61:139-149.

Tucker, C.J. 1979. "Red and photographic infrared linear combinations for monitoring vegetation." *Remote Sensing of Environment*, 8:127-150.

Tucker, C.J. and P.J. Sellers. 1986. "Satellite remote sensing of primary production." *International Journal of Remote Sensing*, 7:1395-1416.

Turner, M.G. and R.H. Gardner. 1991. "Quantitative methods in landscape ecology: an introduction." In *Quantitative Methods in Landscape Ecology*. M.G. Turner and R.H. Gardner, eds. New York: Springer, pp.3-14.

Tyrvainen, L. and H. Vaananen. 1998. "The economic value of urban forest amenities: an application of the contingent valuation model." *Landscape and Urban Planning* 43:105-118.

Verbyla, D.L. 1995. *Satellite Remote Sensing of Natural Resources*. Boca Raton: Lewis Publishers.

Weiss, M. and F. Baret. 1999. "Evaluation of canopy biophysical variable retrieval performances from the accumulation of large swath satellite data." *Remote Sensing of the Environment* 70:293-306.

Werbos, P.J. 1974. "Beyond regression: new tools for prediction and analysis in the behavioral sciences." Ph.D. Thesis, Harvard University, Cambridge, MA.

Westman, W.E., LL. Strong, and B.A. Wilcox. 1989. "Tropical deforestation and species endangerment: the role of remote sensing." *Landscape Ecology*, 3:97-109.

Whelan, R. J. 1995. The Ecology of Fire. Cambridge University Press, New York, New York, USA.

Woodcock, C.E., J.B. Collins, S. Gopal, V.D. Jakabhazy, X. Li, S. Macomber, S. Ryherd, V.J. Harward, J. Levitan, Y. Wu, and R. Warbington. 1994. "Mapping forest vegetation using landsat TM imagery and a canopy reflectance model." *Remote Sensing of Environment*, 50:240-254.

Wulder M.A., E.F. LeDrew, S.E. Franklin, and M.B. Lavigne. 1998. "Aerial image texture information in the estimation of northern deciduous and mixed wood forest leaf area index (LAI)." *Remote Sensing of Environment*, 64:64-76.

Yoshida, T., and S. Omatu. 1994. "Neural network approach to land cover mapping." *IEEE Transactions on Geoscience and Remote Sensing*, 32:1103-1109.

BIOGRAPHICAL SKETCH

Ryan Russell Jensen was born on June 5, 1973, the only son of John R. and Marsha Jensen. Ryan spent his first three years in Los Angeles and then moved with his family to Athens, Georgia, while his father was an assistant professor of geography at the University of Georgia. After four and a half years in Athens, Ryan's family moved to Columbia, South Carolina, where Ryan graduated from Chapin High School in 1990. After high school, Ryan attended Ricks College, in Rexburg, Idaho, where he graduated with his associate degree in computer information systems in 1992. From June 1992 to June 1994, Ryan served as a missionary for the Church of Jesus Christ of Latter-Day Saints in Brazil's Amazon Basin, where he learned the importance of geography to land use/land cover change. Upon returning to the U.S.A., Ryan attended Brigham Young University where he studied geography and graduated in 1996 with a bachelor's degree, and 1997 with a master's. While at Brigham Young University, Ryan married Tricia Lynn Elkins. In fall of 1997, Ryan arrived at the Department of Geography at the University of Florida to work with Dr. Michael Binford studying landscape scale biophysical remote sensing. Upon receiving his Ph.D., Ryan will begin a tenure-track position at Indiana State University in the Department of Geography.

I certify that I have read this study and that in my opinion it conforms to acceptable standards of scholarly presentation and is fully adequate, in scope and quality, as a dissertation for the degree of Doctor of Philosophy.

Michael W. Binford, Chair
Professor of Geography

I certify that I have read this study and that in my opinion it conforms to acceptable standards of scholarly presentation and is fully adequate, in scope and quality, as a dissertation for the degree of Doctor of Philosophy.

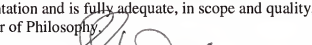

Peter R. Waylen
Professor of Geography

I certify that I have read this study and that in my opinion it conforms to acceptable standards of scholarly presentation and is fully adequate, in scope and quality, as a dissertation for the degree of Doctor of Philosophy.

Nigel J. H. Smith
Professor of Geography

I certify that I have read this study and that in my opinion it conforms to acceptable standards of scholarly presentation and is fully adequate, in scope and quality, as a dissertation for the degree of Doctor of Philosophy.

Cesar Caviedes
Professor of Geography

I certify that I have read this study and that in my opinion it conforms to acceptable standards of scholarly presentation and is fully adequate, in scope and quality, as a dissertation for the degree of Doctor of Philosophy.

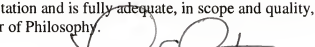

Francis E. Putz
Professor of Botany

This dissertation was submitted to the Graduate Faculty of the Department of Geography in the College of Liberal Arts and Sciences and to the Graduate School and was accepted as partial fulfillment of the requirements for the degree of Doctor of Philosophy.

May 2000

Dean, Graduate School